Published : May 2019

TECHNICAL REPORT

Accident to the Airbus A380 registered F-HPJE and operated by Air France on 30/09/2017 en route over **Greenland**

October 2017 - June 2018
Searches **Phase I & II**

BEA
Bureau d'Enquêtes et d'Analyses
pour la sécurité de l'aviation civile

www.bea.aero

@BEA_Aero

EXECUTIVE SUMMARY

Following the accident to the Airbus A380, registered F-HPJE, during cruise over Greenland on September 30, 2017, the Danish Accident Investigation Board (AIB D) delegated the opening and carrying out of the safety investigation to the BEA. The BEA represents France, State of Operator, State of Registry and State of Design of the aircraft. Investigators from AIB D, representing Greenland (autonomous constituent country of the Kingdom of Denmark), State of Occurrence, from NTSB, representing the United States of America, State of Engine Manufacturers, and BST-TSB, representing Canada, State where the flight crew diverted, took part in this safety investigation.

Four BEA investigators travelled to Goose Bay on Sunday, October 1, accompanied by technical advisors from Airbus and Air France. NTSB investigators, accompanied by technical advisors from the engine manufacturer Engine Alliance (which is a Joint Venture between General Electric and Pratt & Whitney), as well as TSB investigators, also travelled to the site.

A fifth BEA investigator travelled to Ottawa to attend the first read-out of the Cockpit Voice Recorder (CVR) and Flight Data Recorder (FDR).

The Airbus A380-800, operated by Air France, was performing a flight from Paris (France) to Los Angeles (United States of America) under the call-sign AF066. It had taken off from Paris Charles de Gaulle Airport on Saturday, September 30, 2017 around 09:30 (UTC), with 497 passengers and 24 crew members on board. Following a failure on the N° 4 engine while the plane was climbing to FL370, the flight crew diverted to Goose Bay Airport (Canada), where they landed at 15:42 (UTC) without any further incident.

Damage to the aircraft was confined to the N° 4 engine and its immediate surroundings. A visual check of the engine had shown that the fan, first rotating assembly at the front of the engine, along with the air inlet and fan case, had separated in flight.

The data contained in the flight data recorder (FDR) was used to determine the aircraft track and the aircraft position when the failure of the N° 4 engine occurred and to demarcate a search area to find the parts which had separated from the aircraft.

This area turned out to be a wasteland covered with ice, situated about 150 km southeast of the city of Paamiut located on the west coast of Greenland.

The BEA got in contact with its Danish counterpart immediately after the accident to perform a visual search and recovery of these parts.

Quite early in the investigation, it was established that the recovery of the missing parts, especially of the fan hub fragments, was the key to supporting the investigation of the cause of the engine failure.

Search and recovery operations of the fallen parts were expected to be very challenging. The area is remote and weather conditions are extreme most of the year. Soon after the event, some parts were visually spotted and recovered but snowfalls prevented further helicopter flights to the site again. Snow finally covered all the parts that were still lying on the ground, preventing any new visual detection.

Other means of detection then had to be evaluated. These means had to be compatible with the particular conditions of this area, and all their subsequent operational constraints.

It was not possible to go to this region during the winter, as the safety level (cold temperature, short daylight, changing weather, presence of crevasses, etc.) was deemed not sufficient. Therefore, the closest time slot for considering search and recovery operations was Spring 2018.

After a capabilities prospection phase, it was decided to setup two consecutive operations:

- an aerial campaign, consisting in the use of synthetic aperture radars operated from an airplane, to try to detect and locate the missing parts on the ice sheet under the snow layer;
- a ground campaign, consisting in recovering the parts previously located during the aerial campaign, or in performing a systematic search with help of ground penetrating radars in case the aerial phase was unsuccessful.

To face these challenges, a sub-group dedicated to Search and Recovery ("Survey") was set up in the Aircraft Group (see Fig. 1).

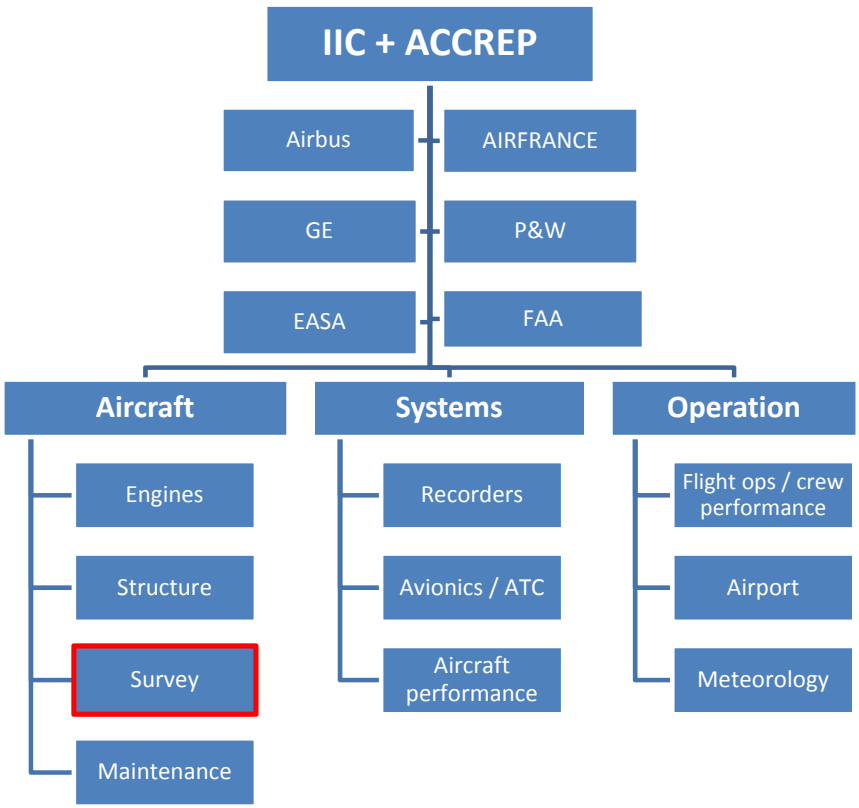

Fig. 1: chart of investigation organization

The purpose of this report is to present the different tasks carried out to prepare and perform the search operations to recover the engine parts. These tasks were the following (see Fig. 2):

- Search Operations
  - PHASE I: rough determination of a search area just after the event and recovery of any visually spotted parts where possible,
  - PHASE II: evaluation of search capabilities and search operations (preparation and performance)
- Search area definition (for PHASE II)
  - ballistic computations
  - engine failure simulation

This report covers the period from the date of the accident to the end of June 2018. This period encompasses Phase I (helicopter flights to recover the debris located just after the event) and Phase II (aerial and ground campaign as well as their preparation), see Fig. 2. In June 2018, a plenary meeting was held with all the parties to debrief the aforementioned search phases. The definition of the search area progressed in parallel, with help of ballistic computations and numerical simulations. Further work is discussed in the last chapter.

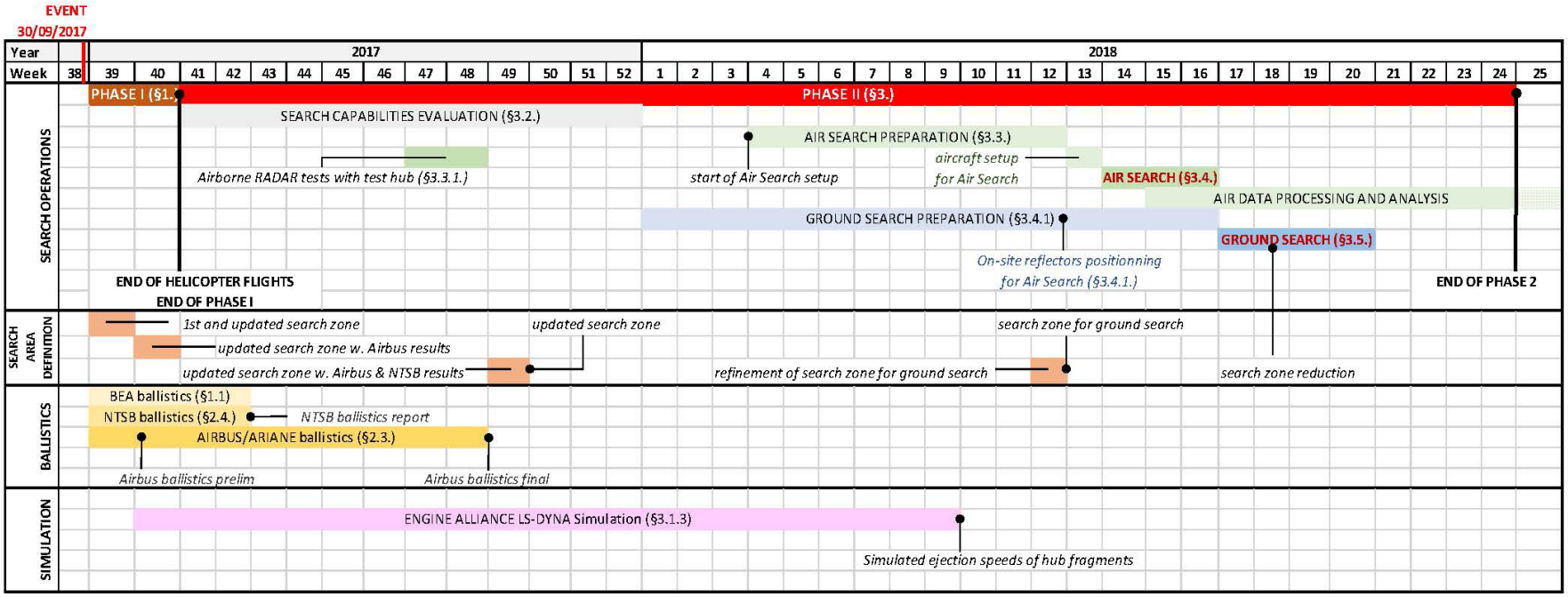

Fig. 2: timetable of search operation, phase I and phase II, from date of accident up to end of June 2018

TABLE OF ILLUSTRATIONS

1 - PHASE I

1.1 Location of event and first recovery actions

On October 2, 2017, AIB-D delegated the investigation to the BEA. The estimated event position was rapidly requested in order to organize search and recovery operations over the ice sheet in Greenland, as the weather conditions at that time of the year can be particularly difficult, with cold temperatures and snowfalls. Therefore it was necessary to launch recovery operations quite quickly in order to recover the parts before any snowfall.

The coordinates of the engine fan module detachment event were provided by the system group from IRS (Inertial Reference System) data first. The exact UTC time of the event was also determined from FDR data, and was commonly agreed to be timestamped at 13:49:18.506 based on the UTC time recorded. The trigger considered for the event was the first peak of lateral acceleration.

No primary radar was available in that region which would have helped to determine the trajectories of the ejected parts.

As the purpose of the Phase I search was to go as quickly as possible, no interpolation was performed on the recorded parameters. The following information was given to the Danish AIB.

61°44'21.91''N / 46°49'1.30''W at 13:49[(1)]
with an estimated aircraft true track: 245°

[(1)]Unless otherwise stated, all GPS coordinates are given in the WGS-84 geodetic system and time is given in UTC (Universal Time Coordinated) time standard.

Priority and secondary search areas were roughly determined by the BEA from basic ballistic computations: the travel distance was estimated by considering the parts as balls without drag, departing at an altitude of 37,000 ft and with an initial speed of 244 m/s.

The priority area was 115 km^2 in surface, and is shown in red in Fig. 3. The secondary area was around 200 km^2 in surface, also shown in Fig. 3, in yellow.

The conical shape of the search areas was determined arbitrarily. It was supposed to take into account uncertainties related to the unknown angle of ejection of the parts when departing from the engine.

The data was given to the AIB-D on October 4, in the morning, and in the afternoon, the AIB D rerouted an ice study helicopter flight to the defined area. Some parts were rapidly visually identified on top of the ice sheet and some were immediately recovered by the helicopter crew. Fifteen fan blade fragments and some composite parts of the cowling were recovered that day.

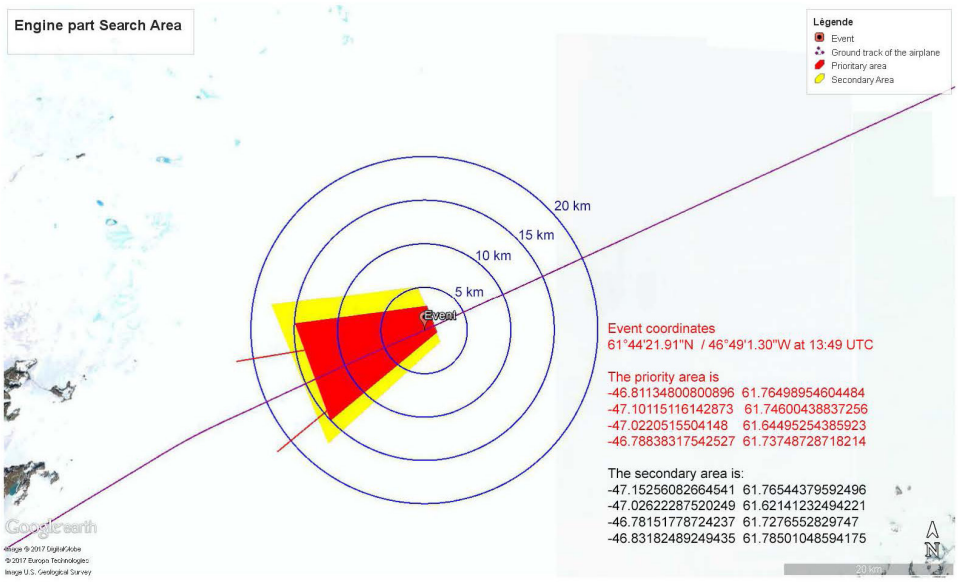

Fig. 3: **priority** and **secondary** search areas

Fig. 4: view of area where first debris was located – straight lines are footprints

On October 5, the track of the AF066 flight was analyzed, which resulted in correcting the event point, moving it 500 m north of its previous position. One of the reason was that the IRS track (from which the event position was first determined) had an offset with runways position. This offset was identified on the runways of both take-off and landing airports (Paris Charles-De-Gaulle and Goose Bay). Given the fact that the FMS (Flight Management System) position is computed from the IRS and the GPS, the BEA decided not to use the FMS position as a second source for locating the event point. It was decided to use the GPS position instead.

Therefore, the GPS track was taken, as it did not present any offset with airports runways. The GPS position at 13:49:19.557 UTC was chosen:

N61°44'43.544'', W046°48'59.724'' at 13:49:18.557

This resulted in a shift of 500 m of the event point to the North and slightly East.

The same day, the BEA received the first pictures of debris from the AIB-D. The debris consisted in fragments of fan blades, spinner, honeycomb, engine pylon, inlet lip, bulkhead, and fan case kevlar belt. A map of the debris was also provided (see Fig. 5). Examples of debris are shown in Fig. 6 and Fig. 7.

Information gathered by the investigation team working on the damaged aircraft in Goose Bay led the team to consider the fan hub of the engine as a priority part to be recovered, in order to support the investigation into the root cause of the event. This information was given to the AIB D as soon as it was received. No fan hub fragment was spotted nor recovered during the first flight.

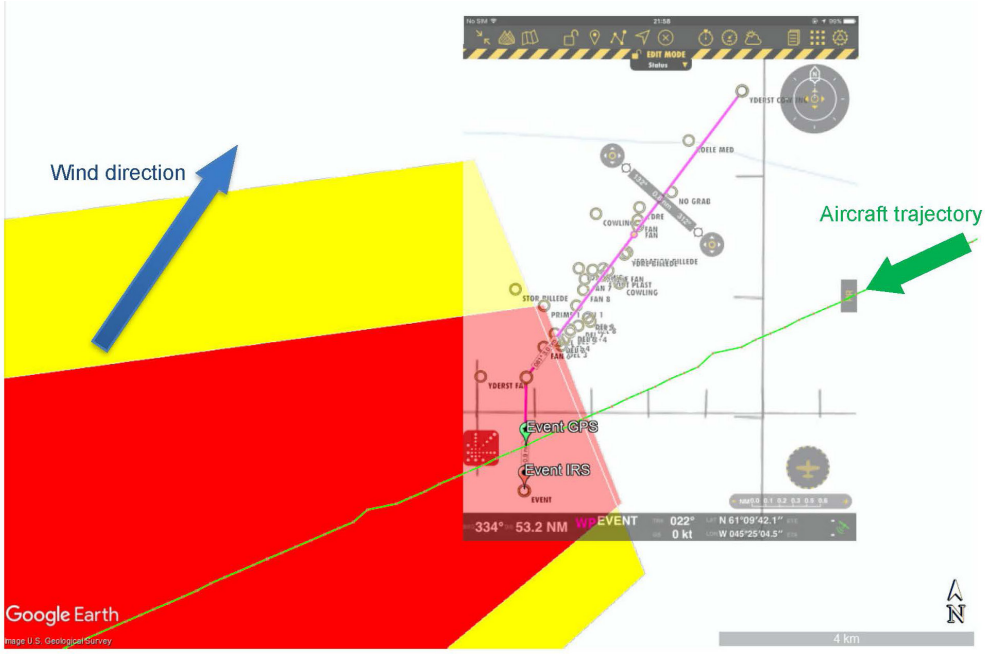

Fig. 5: map of debris located during first helicopter flight

Fig. 6: bulkhead and fan containment case fragment as found on site
(picture courtesy of Air Greenland/AIB-D)

Fig. 7: part of inlet lip photographed on site by an Air Greenland staff member
(picture courtesy of Air Greenland/AIB-D)

The first helicopter flight was carried out on October 4, and until October 8, the weather conditions did not allow another flight to be performed. Weather conditions then improved and on October 8 they were good enough to allow a second flight over the search area. Its track is shown in Fig. 8. This flight resulted in the finding of another blade fragment. No fan hub fragment was found.

On October 11, a last helicopter flight was performed over the area, without any new finding. The helicopter track of this last flight is shown in Fig. 9.

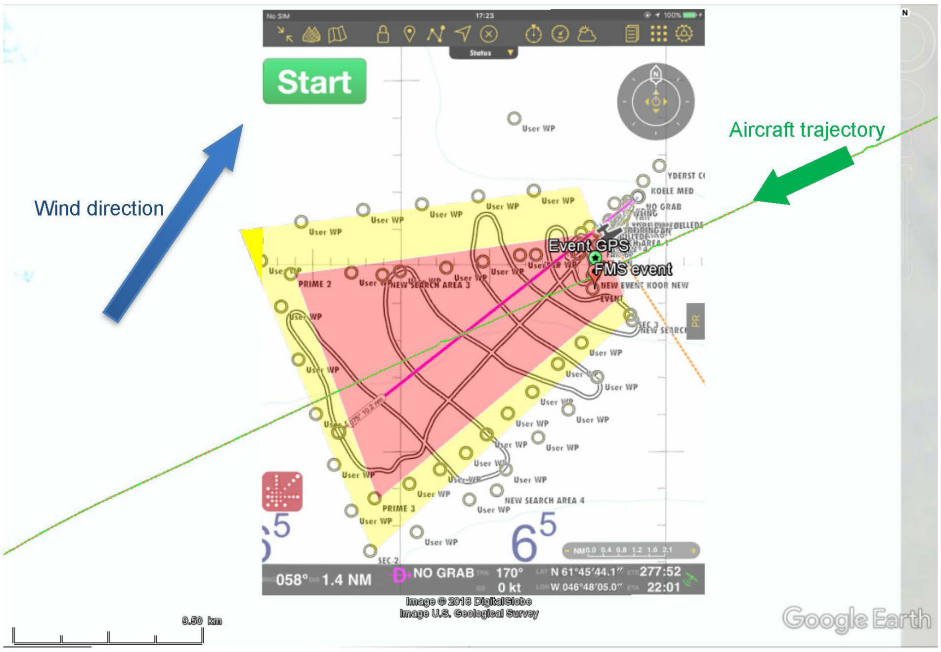

Fig. 8: track of second helicopter flight over search area

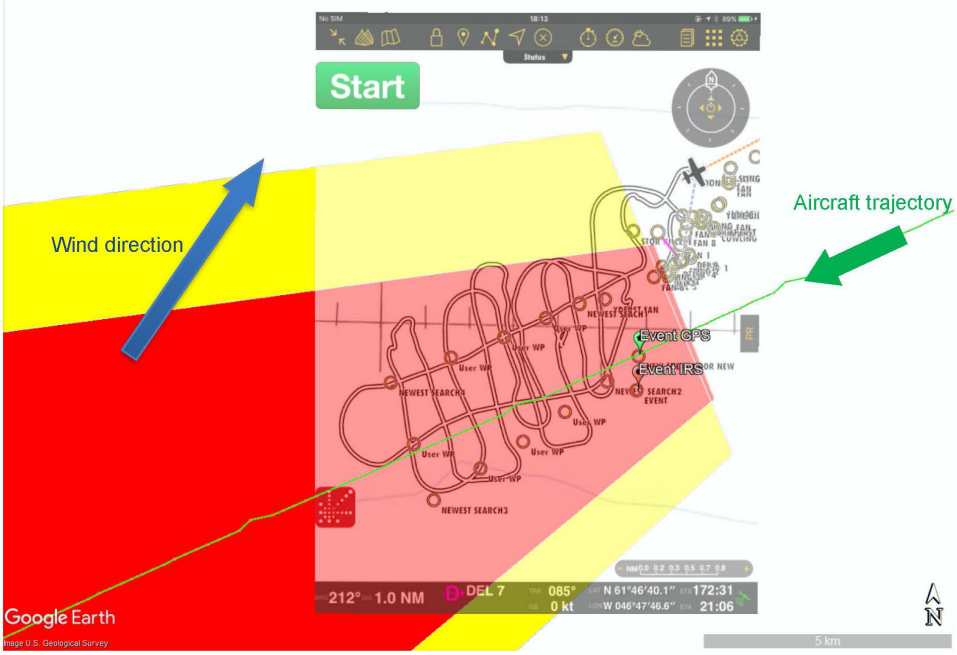

Fig. 9: track of third helicopter flight over search area

As snowfalls and wind had probably covered the remaining parts with snow at that time and did not permit further new visual detections of those still in the area, it was deemed pointless to perform any other flight. The decision was made to end the Phase I. Other methods had then to be investigated in order to locate and recover the missing parts, with a first priority given to the fan hub fragments.

The smallest parts which were recovered during the three visual inspection flights were transported to Narsarsuaq airport. They were stored in a heated and secured hangar. Specific flights on October 12 were necessary to airlift the biggest parts to Narsarsuaq Airport.

A total of 30 parts were recovered. Some of the biggest were precisely GPS-marked:

- N° 1: Bulkhead and fan containment case fragment: N61°45'40.1 W046°48'29.4 (Fig. 10)
- N° 2: Inlet part: N61°45'46.1 W046°47'52.2 (Fig. 11)
- N° 3: Part of composite cowl: N61°45'34.2 W046°48'22.6 (Fig. 12)
- N° 4: Kevlar belt: N61°46'08.9 W046°47'40.4 (Fig. 13)

Fig. 10: inlet cowl aft bulkhead and fan containment case fragment

Fig. 11: inlet part

Fig. 12: part of composite cowl

Fig. 13: kevlar belt

A GPS survey was carried out for all the other parts (see Fig. 5) but there was no way of knowing which part corresponded to what GPS coordinate. The Air Greenland pilots also declared that some of the parts were photographed and GPS-marked, but were finally not recovered. It has to be noted that all the parts recovered were found upstream from the event point, whereas the search area, mainly dedicated to the search for fan hub fragments, was defined downstream from the event point. The reason is that the recovered parts were mainly light parts (composite parts, parts of the nacelle, fan blades). These parts were taken by the wind (wind direction is shown in Fig. 5, Fig. 8 & Fig. 9). This did not lead to the definition of the search area being reconsidered, as the fan hub fragments have probably a higher ballistic coefficient than the recovered parts due to their size, weight and shape.

The parts which could be air freighted were sent to the BEA on October 12 by the AIB-D. They were received at the BEA headquarters on October 25.

The other parts, too big to be air freighted, were shipped on October 22 from Narsarsuaq to Aalborg (Denmark) and then transported by truck to the BEA. They were received at the BEA headquarters on December 12.

1.2 Satellite imagery

Launched in December 2011, the Pléiades constellation is composed of two very-high-resolution optical Earth-imaging satellites. Pléiades-HR 1A and Pléiades-HR 1B provide coverage of the Earth's surface with a repeat orbital cycle of 26 days and daily accessibility to any point of the Earth. Designed as a dual civil/military system, Pléiades meets the space imagery requirements of European defense as well as civil and commercial needs.

Airbus is a partner of this project led by the CNES (Centre national d'Etudes Spatiales).

Airbus deployed the satellites to take images of the search area just after the event. The first images were obscured by cloud cover and the first usable Pleiades images were dated October 11 and 14, the event occurred on September 30. Indeed, to get workable images, two conditions have to be met: the satellite constellation has to pass over the search area, by daylight, and the weather has to be good enough to be able to see the ground (no cloud).

However, given the presence of snowfalls and wind in the search area just after the event, the likelihood of being able to see a piece of debris on the satellite images available at the earliest date (October 11) was very low. Moreover, the dimension of the parts of interest (fan hub fragments) is less than one meter, when the satellite image pixel size is 50 cm (the best reachable resolution is 50 cm).

Even so, October 11 images were looked at, without any findings being made. The only feature spotted is shown in Fig. 14. It corresponded to a helicopter, probably Air Greenland AS350 which was onsite for part recovery that day. One can probably distinguish a man standing by debris, south of the helicopter (Fig. 15).

Fig. 14: Pléiades satellite image of search area, dated October 11, 2018

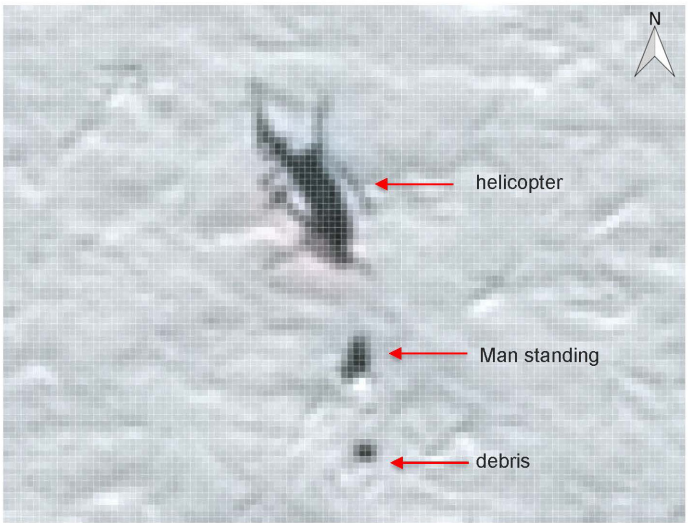

Fig. 15: detail of red box in Fig. 14 - 1 pixel size is 50 cm by 50 cm

2 - SEARCH AREA COMPUTATION

2.1 General data for computation

Once the first phase of search and recovery was over, some parts of interest were still missing. In particular, the fan hub fragments that had become detached were not recovered during Phase I.

The observation of the damage on the engine led the team to consider a fan hub failure as a probable scenario. Moreover, a hub fragment, still attached to the engine, exhibited some fracture surfaces. These fracture surfaces were examined in detail and it was concluded that they were consistent with an overload failure. Therefore, it was of particular interest to try and recover the other fan hub fragments, where the origin of the hub failure would probably be located.

In order to set up a second phase of search and recovery of the missing parts (later called Phase II in this report), it was necessary to determine a limited search area in which there was a high probability of the fan hub fragments being present.

Several calculations were carried out with the following information[(2)]:

[(2)]Recorded FDR values at 13:49:18.557.

Event data:

- ❒ Event coordinate (fan separation) i.e. starting point for calculation: N61.745429; W46.81659 (GPS position recorded at 13:49:18.557)
- ❒ Event pressure altitude: 37076 ft
- ❒ True Airspeed: 483 kt
- ❒ True Heading: 243°
- ❒ Ground altitude: 1842 m

Wind data:

- Wind data on the event day was requested from Météo France. It is presented in Table 1.

Level (x100 ft)	Speed (kt)	Direction
370	27	214°
200	20	214°
150	15	210°
100	10	200°
50	5	180°

Table 1: wind data on day of event

Characteristics of the fragments:
A disk burst usually results in two or three main fragments.

According to the damage observed on the engine, two areas exhibited significant damage consistent with the ejection of fan hub fragments. One was located at the 11 o'clock position on the engine, aft looking forward, the other at the 5 o'clock position (see Fig. 16 & Fig. 17).
These positions were considered as the most probable exit angles of fan hub fragments for the search area computation. The investigation team concluded that there were two main fragments and possibly a third smaller one.

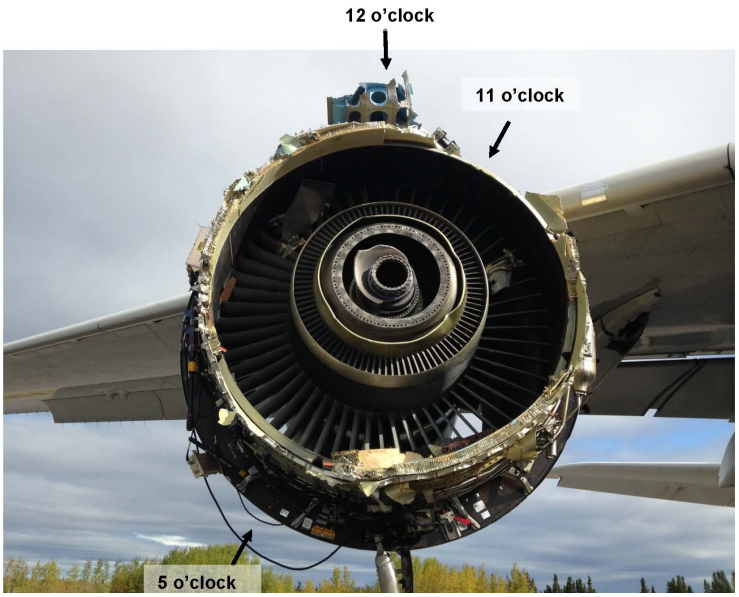

Fig. 16: front view of engine N° 4 on aircraft after landing

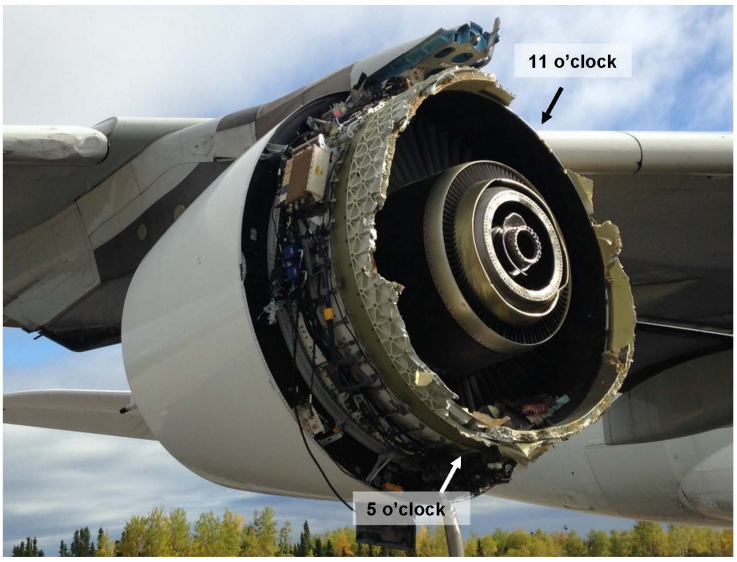

Fig. 17: side view of engine N° 4 on aircraft after landing

What remained unknown was the size and the weight of the fragments, and whether fan blades were still attached to these or not.

The above observations led to fragments of 1/3 and 2/3 of a fan hub being considered for the ballistic computation.

One third of a fan rotor with blades, fairings, pins, and root spacers has a mass of 186 kg (410 lbs), and the Center of Gravity (CG) is located at radius, 584 mm (23.0 in) from the centerline.

One third of a fan hub has a mass of 73 kg (160 lbs) and a CG at radius, 343 mm (13.5 in) from the centerline.

The rotation speed of the hub at the time of the event (around 107 % N1) was 2638 rpm.

2.2 Depth of penetration of hub fragments

Early in the investigation, the AIB D involved GEUS (Geological Survey of Denmark and Greenland[3]) in the discussions as they were well aware of the challenges linked to the environment on site. As part of their involvement, they performed an order-of-magnitude analysis in order to try to determine the impact depth of a hub fragment.

The system can be modeled as a momentum transfer problem. The fan hub fragment will stop when it has transferred all its momentum to the surface of Greenland. As a first approximation, that momentum transfer will be complete once the hub fragment displaces material equal to its own mass (this assumes the ejecta travels out at the same velocity as the incoming object). In reality the snow is not displaced but probably compacted. Because this has the effect of increasing the density of the snow, this would probably reduce the impact depth from the values calculated here.

The height of a cylinder of snow with a mass equal to the fan hub fragment can be solved with:

$$z = \frac{m_{hub}}{\pi r^2 d_{snow}}$$

Where z is the depth of the hub, m its mass, r its radius and d is the snow density. The snow density is of the order of magnitude of 500 kg/m^3. A 75 cm diameter cylinder weighing 225 kg gives a depth of 1 m. Making assumptions about smaller parts leads to shallower depths. To this, one has to add the quantity of snowfalls, which is 1 to 2 m after one winter season.

The total depth of the fragments in the ground should reasonably be 2 to 3 m after one winter season, so in Spring 2018.

This approach was tested with the weight and radius of World War II bombs, the bulk density of soil, and the depth at which they were found from recent newspaper reports, and it appears to work quite well in these scenarios.

2.3 Airbus/Ariane ballistic computation

Airbus took advantage of the expertise of Ariane group in the calculation of ballistic trajectories for launcher debris. Their approach was to look at the exit trajectory of the fan hub fragments on the engine. The lift coefficient and speed of the expelled parts were considered as influencing parameters.

The exit velocities considered for the computation were 20, 50 and 105 m/s. 105m/s was the speed defined as per AMC 20 128A[4] for a third of a disc. 20 and 50 m/s were arbitrary speeds to account for a loss of speed during penetration of the fan case.

The maximum exit velocity was derived using the hub details and engine rotation speed at the time of the event. It did not take into account any energy loss due to hitting other parts of the aircraft.

All radial trajectories were computed, instead of looking at only one or two radial ejection angles.

[3] Refer to http://www.eng.geus.dk/ for more information.

[4] Acceptable Mean of Compliance AMC 20 128A (Design Considerations for Minimizing Hazards Caused by Uncontained Turbine Engine and auxiliary Power Unit Rotor Failure) sets forth a method of compliance with the requirements of CS 23.901(f), 23.903(b)(1), 25.903(d)(1) and 25A903(d)(1) of the EASA Certification Specifications (CS) pertaining to design precautions taken to minimise the hazards to an aeroplane in the event of uncontained engine or auxiliary power unit (APU) rotor failures. The guidance provided within this AMC is harmonised with that of the Federal Aviation Administration (FAA) and is intended to provide a method of compliance that has been found acceptable. As with all AMC material, it is not mandatory and does not constitute a regulation.

For each condition, 500 impact points were computed, scattering in a uniform manner the ballistic coefficient and the lift/drag ratio (0 to 2%) of the fragment.

Fig. 18 to Fig. 21 show the distribution of the results depending on the angle of ejection, speed and lift/drag ratio, for a fragment of 1/3 of a hub. Angles of ejection are presented in different colours: yellow stands for the 5 to 9 o'clock position aft looking forward, blue for 9 to 1 (9 to 12 then 12 to 1) o'clock and red for 1 to 5 o'clock. Fig. 21 is an overlay of all the computed speeds of ejection.

Calculations were also made for a fragment of 2/3 of a fan hub exiting the engine at the 11 o'clock position, aft looking forward, with an ejection speed of 0 and 105 m/s and lift/drag ratio from 0 to 5%. The computed points are shown in Fig. 22.

From the computations, it can be noted that a larger fragment (2/3 of a fan hub for example) will fall further west than a smaller one for the same lift/drag ratio.

The resulting search surface, shown in Fig. 23 in red, encompasses the computation results for 1/3 and 2/3 of a fan hub and extends over 8.3 km^2. It was defined considering that an angle of ejection at 3 o'clock was not consistent with the damage observed on the engine. In the same way, no damage was observed on the fuselage so an angle of ejection of 9 o'clock was very unlikely. Therefore, the northern part of the blue and yellow points as well as the southern part of the red points were eliminated.

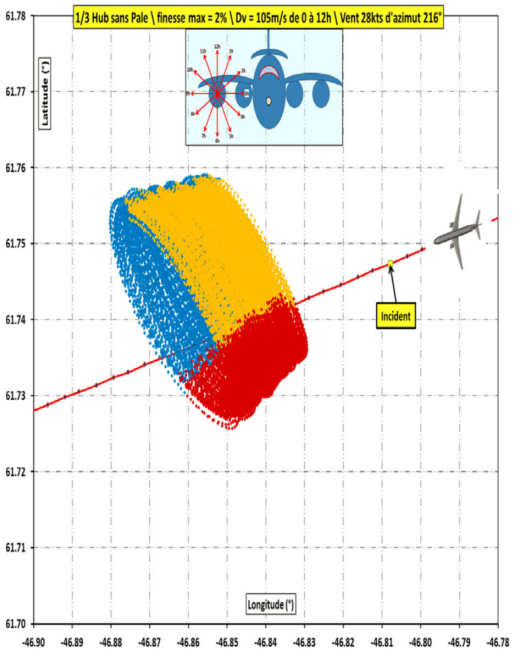

Fig. 18: 1/3 of a fan hub with an ejection speed of 105 m/s (courtesy of Arianegroup)

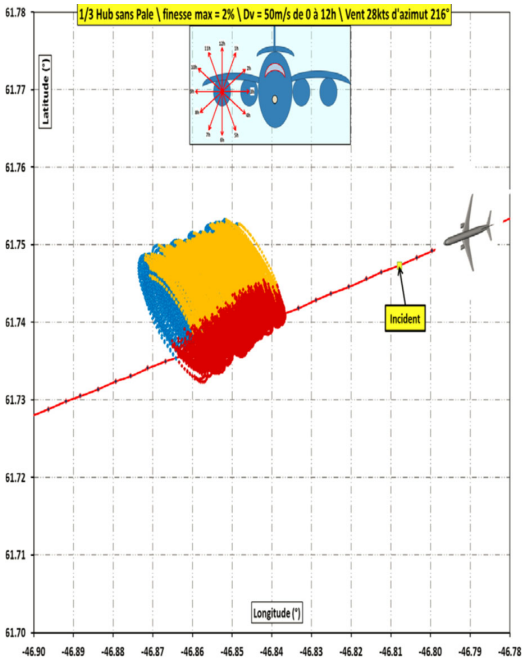

Fig. 19: 1/3 of a fan hub with an ejection speed of 50 m/s (courtesy of Arianegroup)

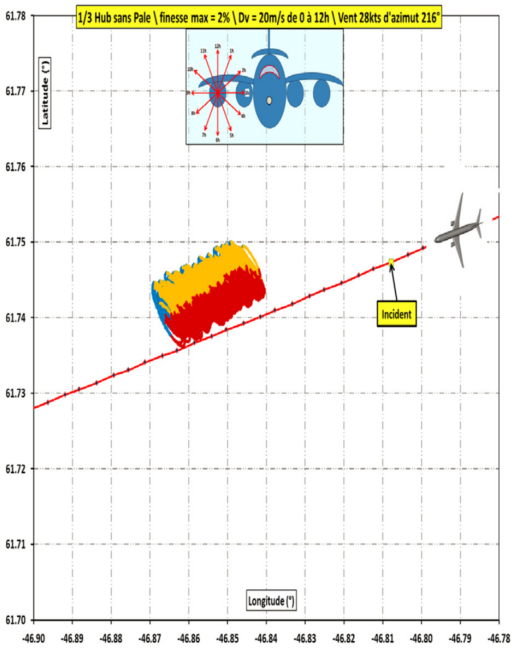

Fig. 20: 1/3 of a fan hub with an ejection speed of 20 m/s (courtesy of Arianegroup)

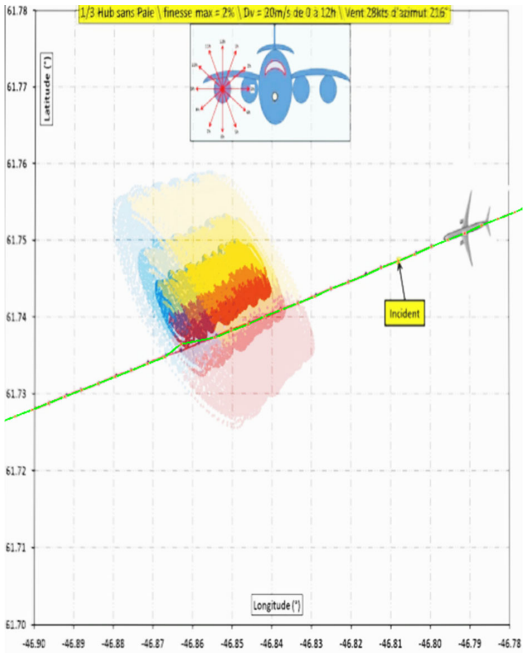

Fig. 21: overlay of the 3 computed ejection speeds for 1/3 of a fan hub (courtesy of Arianegroup)

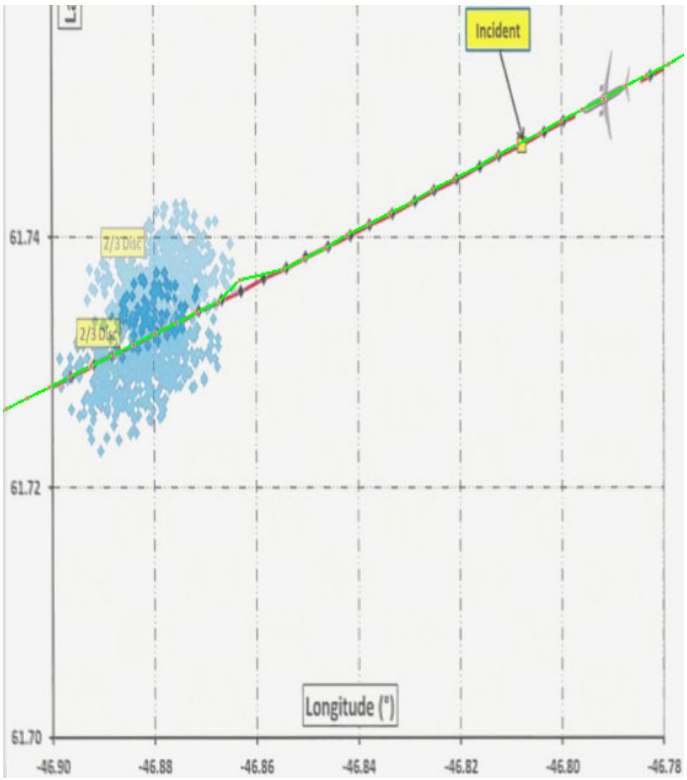

Fig. 22: impact location computations for 2/3 of a fan hub
with an ejection speed of 0 and 105 m/s at 11 o'clock, lift/drag ratio from 0 to 5 %
(courtesy of Arianegroup)

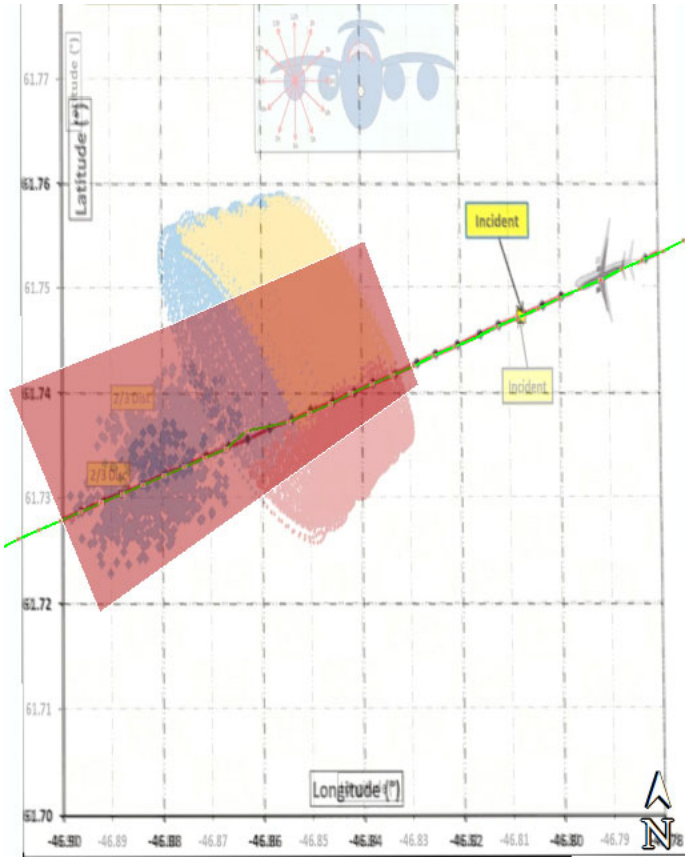

Fig. 23: search area considered after Arianegroup computation. Northern blue and yellow points correspond to the 3 o'clock ejection angle, which was not consistent with damage on the engine. Southern red points correspond to the 9 o'clock ejection angle (toward the fuselage), not consistent either

2.4 NTSB ballistic computation

If given an exact ballistic coefficient of an object, the exact initial conditions and the atmospheric conditions, it is possible to predict exactly where this object will fall. But in general, such exact data is not available. In this specific case, initial conditions such as the event position (latitude/longitude) and altitude, the aircraft track angle, the aircraft ground speed, its flight path angle, the rotation speed of the engine and the winds at time of the event are key. Also, the shape and weight of the part play a significant role in determining the ballistic coefficient. As these were not fully established, the NTSB used a range of ballistic coefficients that aimed to cover the variation in size and shape of the hub fragments.

The ballistic coefficient used by the NTSB is defined by:

$$\beta = \frac{W}{C_D S}$$

Where W is the weight of the fragment, C_D is the drag coefficient and S is the "*cross-section area*". The whole methodology used to solve the ballistic equations is presented in (Crider, 2015).

Assuming constant wind during the fall (27 kt, 214°) led to the curve in Fig. 24. In this diagram, points 1 to 4 were the recovered pieces of debris presented in paragraph 1.1:

- N° 1: Bulkhead part: N61°45'40.1 W046°48'29.4
- N° 2: Inlet part: N61°45'46.1 W046°47'52.2
- N° 3: Part of composite cowl: N61°45'34.2 W046°48'22.6
- N° 4: Kevlar belt: N61°46'08.9 W046°47'40.4

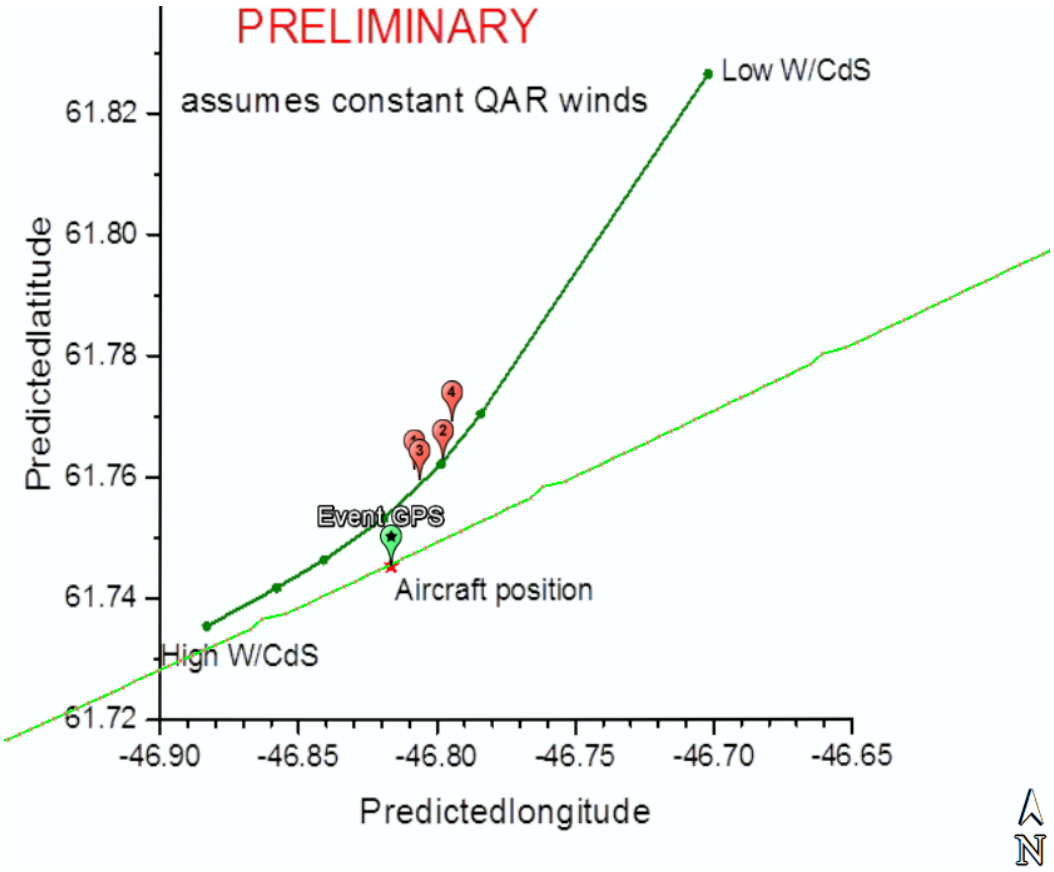

Fig. 24: ballistic locus considering constant wind, with no ejection angle (courtesy of NTSB)

The northeast end of the curve approaches the wind direction while the high ballistic coefficient end of the curve (southwest) approaches the initial track angle or path.

This curve does not take into account any ejection angle from the engine.

The wind was then adjusted to 200° below FL100 for a better match with the debris location.

The velocity of the part relative to the engine should also be added to the aircraft velocity. Any energy loss due to the collision of the part with other aircraft structures can also vary from small to very significant. If the energy loss is significant, the position will be closer to the nominal ballistic locus of Fig. 24.

Physical evidence on the engine indicated departure angles of the fragments at 5 and 11 o'clock positions, aft looking forward.

This adds ballistic locus segments as shown in Fig. 25. The length of the locus reflects the range of estimated ballistic coefficients for the fragments. A range of ballistic coefficients that covered variation in size/shape between the two fragments was considered. The 3 o'clock and 9 o'clock exit angles were used to bracket the problem with a pure sideways departure from the airplane (9 o'clock is not realistic as no fragment hit the fuselage).

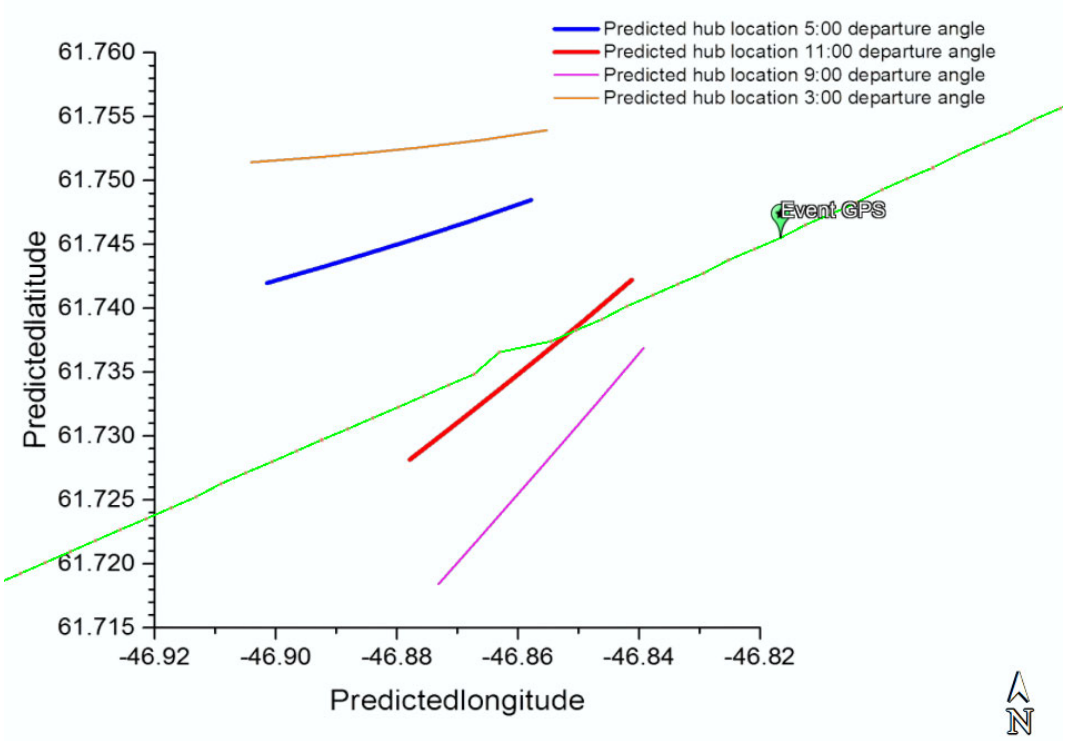

Fig. 25: predicted hub fragment location vs departure angle (courtesy of NTSB)

Fig. 26 shows the paths of the low and high ends of the ballistic range that were used for both the 5 o'clock and 11 o'clock engine exit angles.

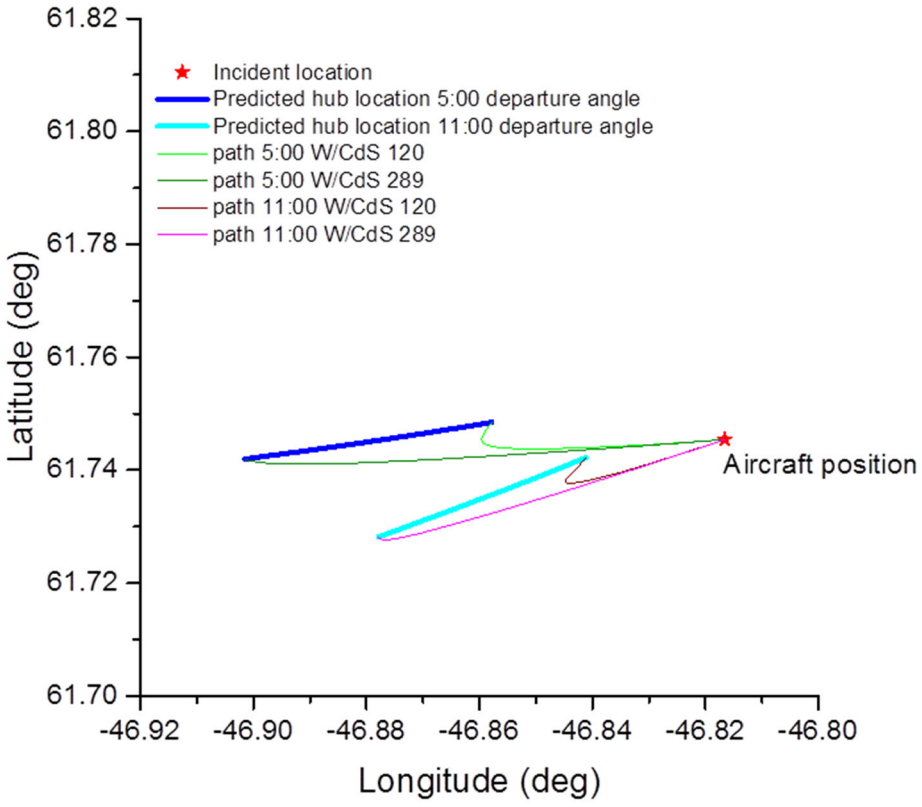

Fig. 26: effect of ballistic coefficient range on predicted hub location (courtesy of NTSB)

Some uncertainty in the angle of exit was considered to determine two primary search areas, see Fig. 27. The loss of energy is taken into account with the secondary area, as 100% of loss of energy would result in the ballistic locus presented in Fig. 24.

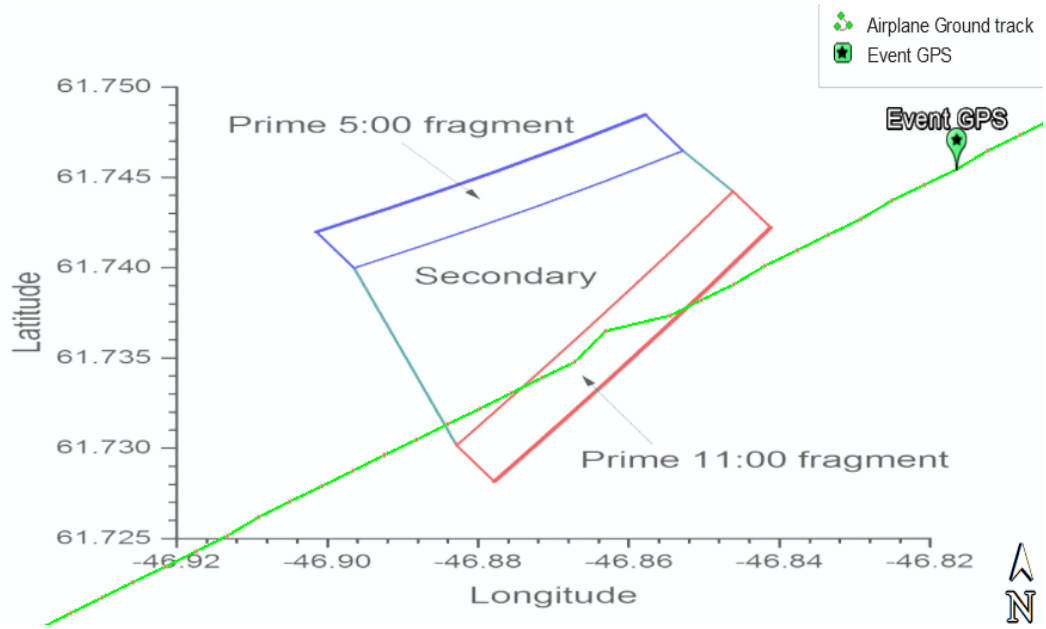

Fig. 27: NTSB primary and secondary areas (courtesy of NTSB)

In total, prime areas extend over 0.68 and 0.84 km^2 for the 5 and 11 o'clock positions respectively, and the secondary area extends over 2 km^2, for a total of 3.52 km^2.

2.5 Search area definition for Phase II

For the preparation of Phase II search operations, a high probability search area was defined in order to determine the most appropriate means for the survey.

An overlap of NTSB and Airbus computations was displayed, leading to the search area presented in Fig. 28. This red box can be divided into two parts: the southern part is deemed as the most promising area with regards to the computations, as most of the calculation results stand in this area. The northern part is an extension of the southern part, encompassing the highest ejection speeds of the Airbus computation.

The total box is 12 km², while the southern part is 7 km² and the northern part, 5 km².

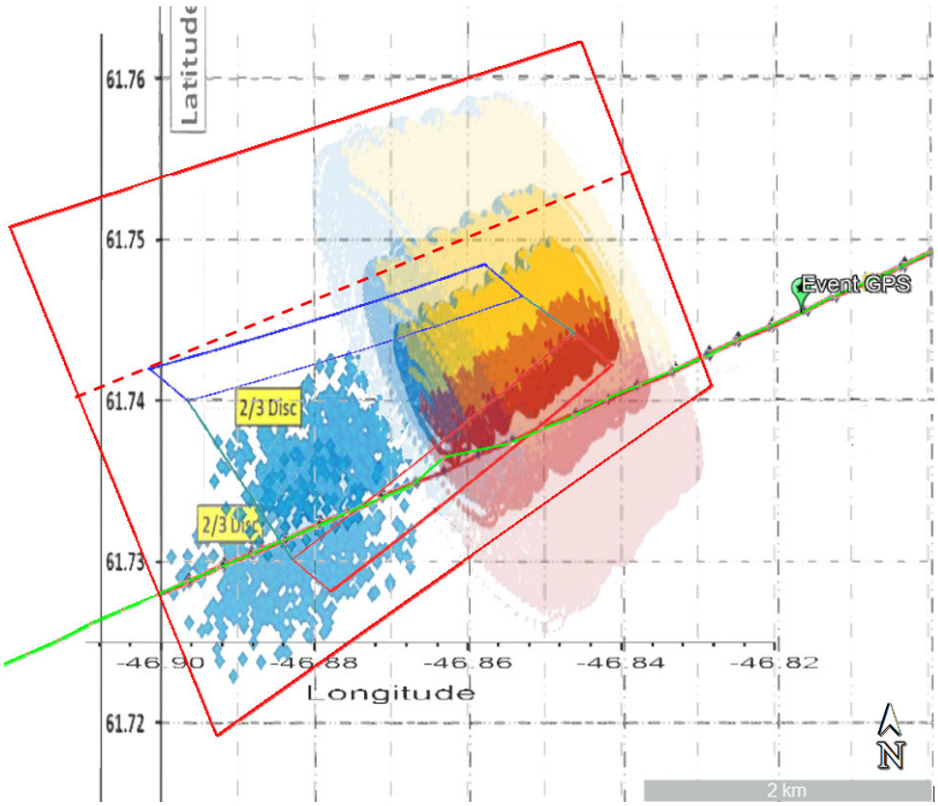

Fig. 28: search area (red box) encompassing Ariane ballistic computation (*1/3 and 2/3 hub*), and NTSB computation

3 - PHASE II

3.1 General

3.1.1 Objectives

The main objective of the Phase II searches was to recover the fan hub fragments which fell on the Greenland ice sheet. It was determined from observation of the damage on the engine that the most probable accident scenario was a fan hub failure which led to the fan module separating from engine N° 4. It was deemed essential to recover the parts to be able to determine the origin of the failure.

3.1.2 Environment

Fig. 29: recovering debris on ice sheet, October 2017. Photo courtesy of Air Greenland/AIB-D

The area where the parts fell is remote, and its environment is hostile. It is an ice sheet with an ice thickness of 800 m, a surface elevation of approximatively 1°800 m and an annual snowfall rate which reaches an average of 1.5 m to 2 m. Temperatures are likely to be below -20 °C from November to April, and daylight during that period is given in Table 2.

	Sunrise UTC	Sunset UTC	Available daylight
November 1	10:45	19:10	8:25
December 1	12:05	18:00	5:55
January 1	12:30	18:00	5:30
February 1	11.35	19:20	7:45
March 1	10:10	20:40	10:20
April 1	08:35	22:00	13:25

Table 2: daylight in search area, November to April

Overall, an ice sheet can be seen as a conveyor belt (see Fig. 30): it is essentially a mass transport system.

The equilibrium line is a virtual demarcation between the accumulation zone (where the ice sheet is gaining mass) and the ablation zone (where the ice sheet is losing mass).

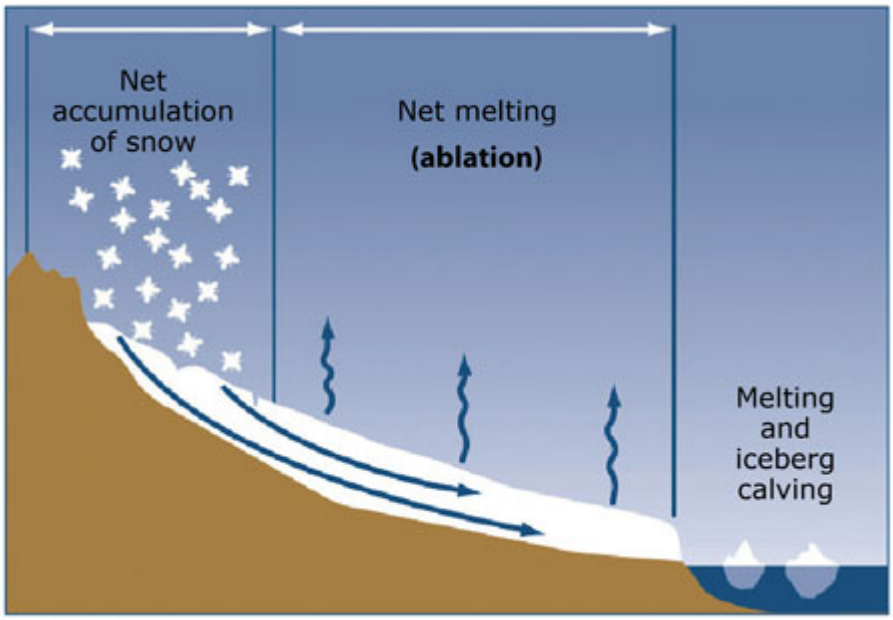

Fig. 30: scheme of an ice sheet (Edward Josberger)

A more detailed look at the accumulation zone (Fig. 31) shows that snow accumulates in a "dry snow zone", at very high altitudes, where the average annual temperatures are below -25˚C. At lower altitudes where temperatures can be higher, water may melt at the surface and percolate down through the snow and refreeze, leading to a warming of the snow. The amount of melt increases as the altitude decreases. This zone is called a percolation zone. A decreasing altitude and increasing temperature can lead to all the snow being at melting point with melt water percolating down to older layers without refreezing. This is the wet snow zone. When the amount of meltwater is so large that there is no snow left but ice, it is known as the superimposed ice zone.

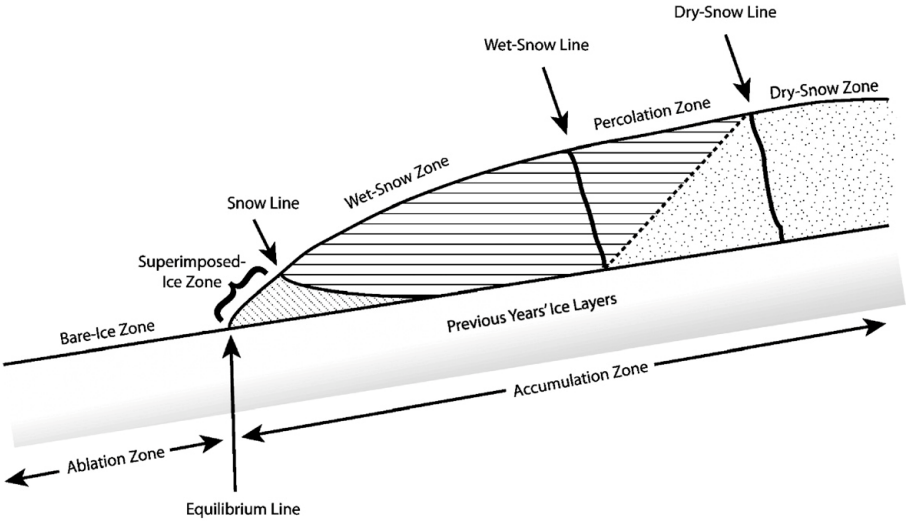

Fig. 31: zoom on accumulation zone on Greenland ice sheet (Benson, 1962) (Paterson, 1994)

The area where debris was recovered is a percolation zone, which is part of the accumulation zone. Once a part is covered by snow, it will not reappear on the surface, even after the summer and melting events. Snow will accumulate above the part with time, meaning that the longer it lies on site, the deeper under the snow it will be.

Moreover, the snow pack is a multilayer of dry snow, wet snow and refrozen water. The properties are highly variable on multiple spatial scales as well as in time, and will affect the reflection strength and the penetration depth of a radar signal.

As a mass transport system, the ice sheet is moving slowly. Ice flow velocities are estimated to be between 39 m to 45 m per year in the area concerned.

More particularly, the area is within 5 km of a faster flowing region and strain rates probably exceed 1%, the theoretical threshold value for the formation of crevasses (see Fig 26). It turned out that there were in fact many crevasses in this region (see paragraph 3.4.3), and their existence is probably due to the subglacial topography. As the ice flows over buried mountain-tops, strain rates increase and crevasses form. (see Fig. 32).

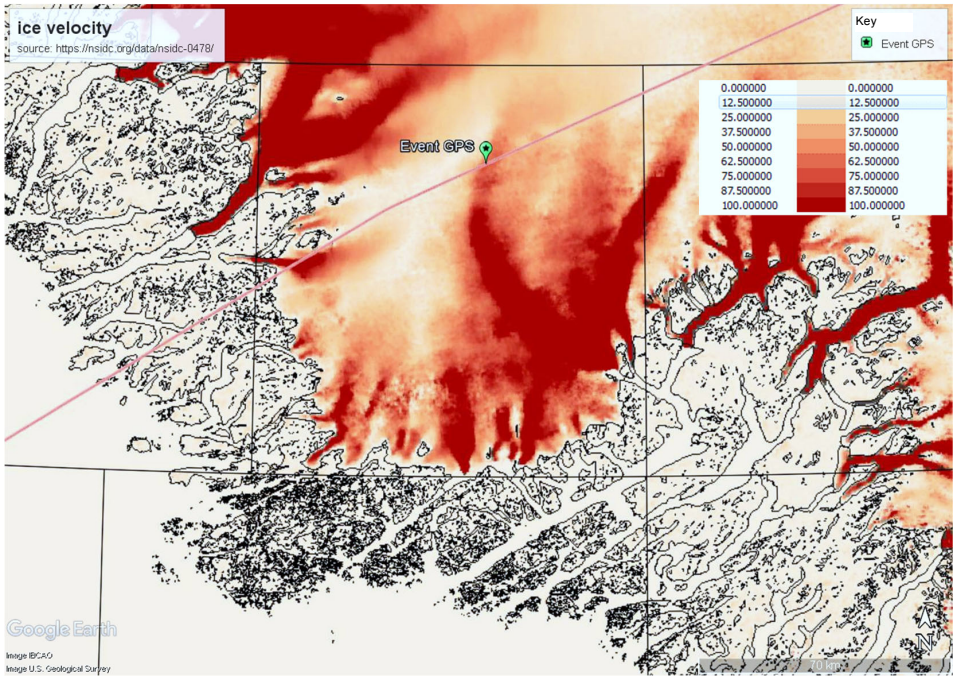

Fig. 32: ice flow velocity map[5] (Joughin I. B., 2015, updated 2018) (Joughin I. B., 2010) velocity range given in m/year – actual velocities can reach 3000 m/year

[5] https://nsidc.org/data/nsidc-0478/

3.1.3 Description of missing parts

The entire fan hub weighs 238 kg (525 lbs). Its diameter is around 34 in (86cm), and the axial length is approximately 23 in (58 cm).

A fragment of 18 kg was still attached to the LPT (Low Pressure Turbine) shaft and recovered by the BEA during the on-site examination, leaving 220 kg still missing.

As part of the investigation, laser 3D scans were carried out on the recovered part of the hub and on an intact hub. This allowed, by subtraction, to assess the shape of the missing part(s) (see Fig. 33).

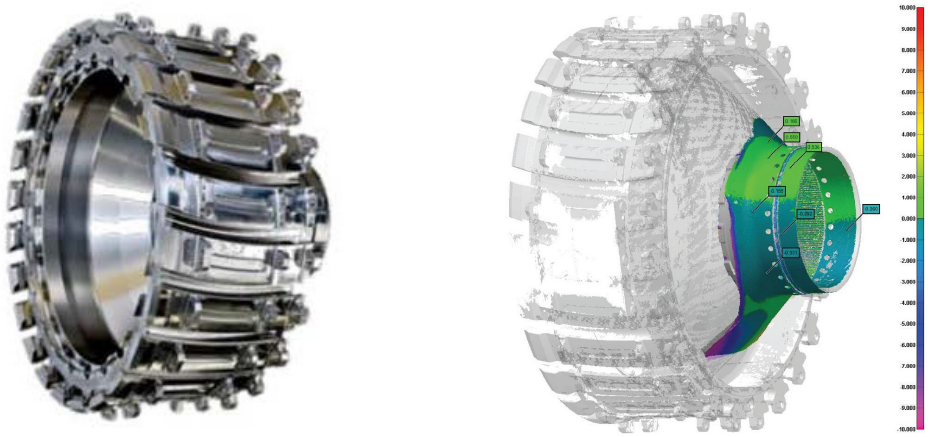

Fig. 33: intact exemplar fan hub (left picture) – recovered part from F-HPJE (in color, right picture)

Damage on the engine exhibited two areas of potential ejection of the hub fragments: one located in the 5 o'clock position, aft looking forward, and the other in the 11 o'clock position. Moreover, a LS-Dyna simulation was performed by the engine manufacturer, Engine Alliance (Fig. 34). It showed that the hub would have separated into two parts if the fan hub body ruptured. According to the simulation, one fragment would weigh 91 kg and the other 127 kg. This is consistent, with a 2 kg error, with the size of the hub remnant found attached to the shaft.

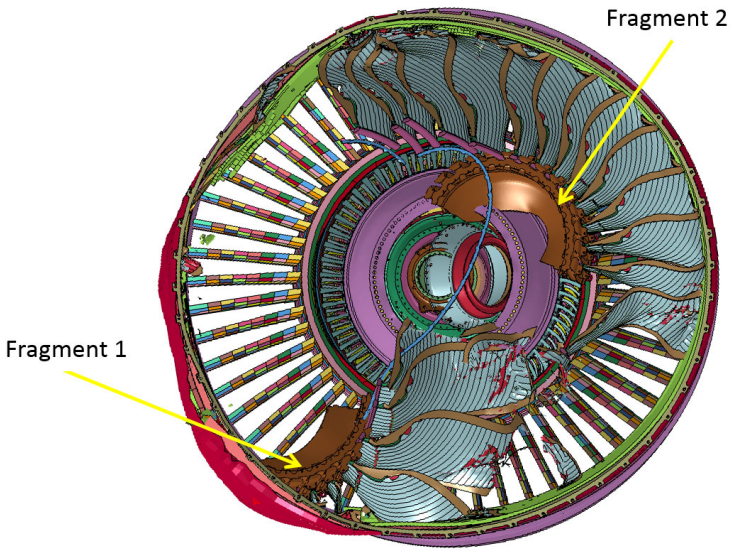

Fig. 34: LS-Dyna fan hub failure simulation (picture courtesy of Engine Alliance)

3.2 Search capabilities

Search capabilities were looked for after the event, as soon as it was known that the parts had fallen on an ice sheet. Once the snow covered the remaining debris, meaning that a visual search was no longer possible (end of Phase I), this task became of first priority. The evaluated capabilities had to be able to detect at least a fan hub fragment 1/3 in size of the hub, up to 2 meters under the snow, taking into account the challenging conditions in the area.

Several techniques were considered: radar imagery, ground penetrating radars (GPR), electro-magnetic detection systems (EM), and synthetic aperture radars (SAR). Some of the systems could be operated on ground or from the air, each option having pros and cons.

3.2.1 Radar Imagery

Airbus evaluated the option of getting TerrasarX[6] imagery for fan hub fragment detection. At the time of the event, the statement from Airbus was that "*due to its characteristics it is very difficult for TerrasarX to penetrate snow/ice. Furthermore the metal pieces seem too small to be detected reliably*".

This solution was not investigated further at that time.

3.2.2 Electro-magnetic detection systems

As the fan hub is made from a titanium alloy, ferro-magnetic detection systems were out of the scope. Electro-magnetic conductivity meters were deemed more appropriate. They can be towed by cars, quads, or even skidoos. The detection distance can extend up to 3 meters on each side. DualEM[7] or Geonics[8] are examples of companies providing such equipment.

A company called Georeva[9], specialized in geophysic instrumentation, operates EM equipment such as the EM31-MK2 or the DUALEM 21s. They were then approached to assess whether these sensors were able to detect titanium parts. Georeva actually did some tests with stainless steel parts that were supposed to have a much better response than titanium parts. These tests were mainly non-conclusive with EM equipment, as the response was qualified as "*versatile*". According to their geophysicist, GPR would be more appropriate for detecting titanium parts under snow.

Fig. 35: example of operation of EM31-MK2 in icy conditions

[6] Refer to https://www.intelligence-airbusds.com/terrasar-x/ for more information.

[7] Refer to http://www.dualem.com/ for more information.

[8] Refer to http://www.geonics.com/ for more information.

[9] Refer to http://www.georeva.eu/ for more information.

3.2.3 GPR operated from the air

The Institute for Geosciences and Environmental research, Grenoble, France (Institut des Géosciences de l'Environnement, IGE[10]) is a fusion of several French academic research laboratories including the Laboratory of Glaciology and Geophysics of the Environment, Grenoble (Laboratoire de Glaciologie et de Géophysique de l'Environnement, LGGE). This laboratory performed geophysical measurements over different areas in the Mont-Blanc massif and in particular over the Argentière glacier. The objective was to map the rock topography of the glacier. To do this, they used the services of a company called RST[11], operating airborne GPR slung under a helicopter.

The main characteristics of the system are the following:

- It allows detection of parts greater than 1m in size, up to 50 m deep.
- The antenna weighs 170 kg, it needs to be operated with low wind, no faster than 30 km/h.
- Track separation is 10 m.
- There is a "*blind zone*" effect that prevents seeing any feature located between the surface and 1.5 to 3 m deep.

Considering the size of the hub fragments, probably smaller than 1 m in size, and the depth of their probable location (around two to three meters below the snow layer), this solution was deemed not appropriate.

Fig. 36: Hera-G radar system (RST) operated by helicopter

Use of drones was also considered, as companies propose GPR operated by unmanned drones such as MGT (Mobile Geophysical Technologies[12]) but taking into account the weather conditions on the ice sheet (strong winds and rapidly changing weather), it was not considered an effective solution in a first approach.

[10] Refer to http://www.ige-grenoble.fr/ for more information.

[11] Refer to http://www.rst-group.biz for more information.

[12] Refer to http://www.mgt-geo.com/ for more information.

3.2.4 GPR operated on ground

Early after the event, the AIB-D contacted GEUS, Geological Survey of Denmark and Greenland[13], as they have experience regarding ice studies and arctic conditions. GEUS is quite used to working with GPR to characterize ice and snow on the ice sheet. This solution was therefore fairly immediately on the table after the event. Even if a GPR is mainly used to detect crevasses or to characterize snow layers on the ice sheet, they are also used for archeological purposes or for the detection of buried objects such as pipes for example.

A GPR can be towed by a vehicle (quad, car, skidoo) or by manpower, walking or skiing. The scanned area depends on the radar size, but needs dense sampling, with long acquisition time and large volume of data, as it only looks below and not to the side. It can be operated at different frequencies, depending on the features that are being looked for.

[13]Refer to http://www.eng.geus.dk/ for more information.

3.2.5 Airborne SAR

The BEA was informed by the French Geographic Institute (IGN) that ONERA (Office National d'Etude et de Recherche Aerospatiale), the French Aerospace laboratory[14], operates a synthetic aperture radar (SAR) system called SETHI.

SETHI is an airborne system developed by ONERA, integrating various sensors. Radar components cover VHF-UHF to X Bands, in a full polarimetric configuration with very high resolution, have along track and cross track interferometry and a very high precision multi-baseline capacity for interferometry and tomography applications.

[14]Refer to https://www.onera.fr/ for more information.

Launched in 2007, the SETHI project is based on an adapted Falcon 20 jet aircraft (Fig. 37). This aircraft, rented from a private company called AVDEF, an Airbus subsidiary and located on Nîmes Garons Airport, has been adapted to accommodate two under-wing pods, about three meters long and 300 kg each.

Fig. 37: AVDEF Falcon 20 F-GPAA

Radar bands operated on the SETHI system are UHF, L and X bands, with polarimetry capability. The UHF radar is integrated in the left pod (Fig. 38) and the X+L radars are in the right pod (Fig. 39).

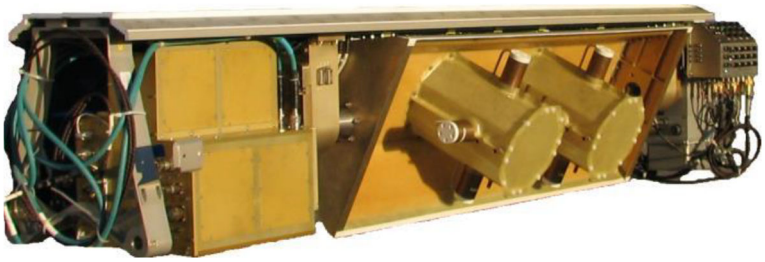

Fig. 38: UHF radar integrated in left pod

Fig. 39: X band radar payload (right) and L band (left) integrated in right pod

Radar	UHF	L	X
Center frequency	340 MHz	1,3 GHz	9,5 GHz
Bandwidth	240 MHz	150 MHz	720 MHz
Resolution	62.5 cm	1 m	20 cm
Polarization	Full (H+V)	Full (H+V)	Full (H+V)
Antenna Beamwidth (site)	80°	31°	16°
Emitted power (peak)	500 Wc	300 Wc	200 Wc
Emitted power (mean)	100 W	60 W	30 W

Table 3: radar parameters

During measurements, the UHF and L bands can be operated simultaneously in a left-looking configuration. In the same way, X and L bands are also associated for simultaneous measurements in a right-looking configuration. The associations X+L+UHF do not operate at the same time but from one measurement to the next. It is also possible to change the depression angle (angle between horizontal and line of sight of the signal) of the X and L components between two measurements. The flight configuration is generally in a linear trajectory but a circular trajectory can also be proposed in order to observe the ground over different azimuth angles.

The swath is directly linked to the altitude above ground and the depression angle (see Fig. 40).

X bands are generally operated 8200 feet above ground, and the resulting ground swath is 3795 m.

L and P bands are generally operated 12000 feet above ground and the resulting ground swath is 5748 m.

This range of swaths would allow coverage of the whole search area with only one flight pass.

As this solution seemed to precisely meet the needs, ONERA was contacted for preliminary tests of their capabilities.

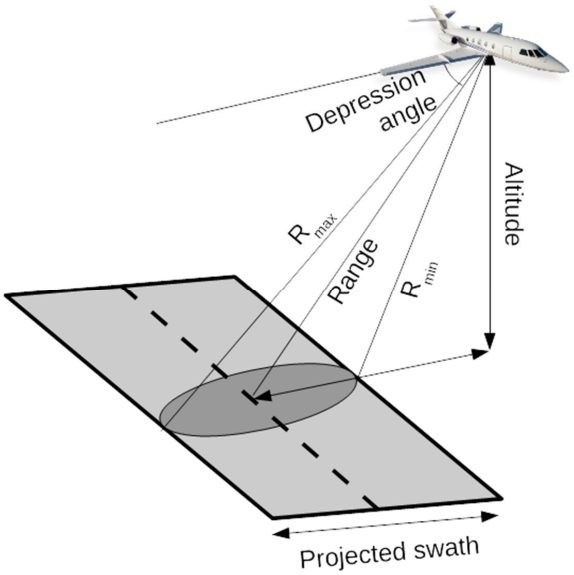

Fig. 40: schematics of side looking radar parameters

3.3 Setting up the PHASE II search campaign

3.3.1 Detection: airborne radar test campaign

The BEA asked ONERA to evaluate the capabilities of the experimental radar platform SETHI to detect and localize fan hub fragments from F-HPJE which are covered by snow in South-Greenland.

In November 2017, a similar fan hub to the event hub was made available to the BEA by Safran Aero Boosters (formerly Techspace Aero), the machining source for the finished part. It was intact and therefore not representative in shape to a fan hub fragment from the event. However, as a first step it was deemed sufficient to use this hub as a test piece and try to detect and locate it with the ONERA SETHI radar. Moreover, the test operation was opportunistic and it would have taken too much time to machine the hub into several pieces just to be closer in shape to the event fragments. A scrapped fan blade provided by Air France was also used as a target for the detection test.

The testing operation was carried out at Nîmes-Garons Airport, from the end of November to mid-December 2017. As it was an opportunistic test, there was no possibility of burying the parts in snow or ice. The parts were simply positioned on a taxiway of the airport (Fig. 41) which was not representative of the situation to be encountered in Greenland. But the possibility of carrying out this test at such short notice was unexpected and very beneficial. The effect of snow and/or ice on the radar response was not evaluated during these tests but they were nevertheless estimated from available scientific literature (see paragraph 3.3.2).

Fig. 41: a fan hub and a fan blade on Nimes-Garons airport for detection testing

The tests resulted in the detection of the fan hub and the fan blade with L, P and X bands (Fig. 42). However, X and P bands gave the best results in terms of contrast, while the L band seemed to be less effective.

On the radar images, all man-made features have a strong bright response. As a reminder, on the Greenland ice-sheet, the only man-made feature would be the parts which are being looked for. The detection of these features would be much easier than the images of Fig. 42, where the test hub and the test blade are very close to lots of man-made infrastructures.

Regarding the difference between an entire hub and hub fragments, ONERA's assessment was that even if hub fragments are smaller, the geometry of the parts, with many sharp edges (blade slots), is still favorable to a strong backscatter and should behave like a point target rather than a distributed target.

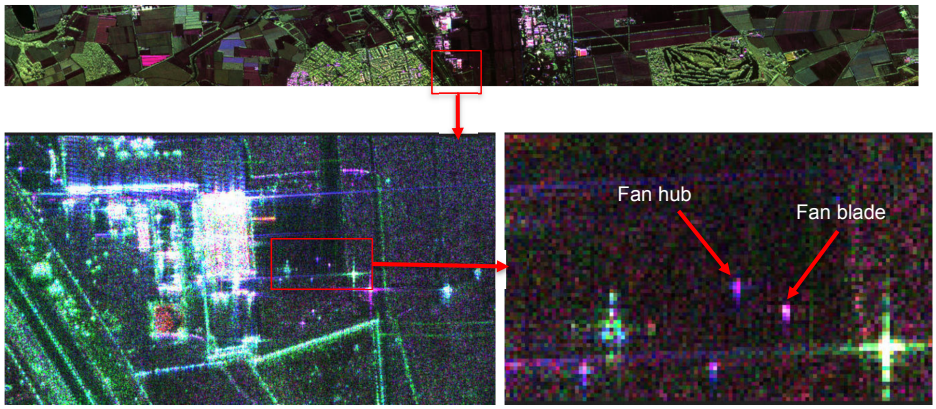

Fig. 42: L-band images, flight heading 270°, full polarization, depression angle 45°, resolution 90 cm x 90 cm

3.3.2 Behavior of SAR in snow and ice

One of the remaining uncertainties was the behavior of SAR in snow and ice. ONERA did a feasibility study based on literature and available radar data over Greenland.

They first estimated the backscatter of the ice sheet, using TerraSAR-X images dated 2015 provided by Airbus (for the X-band), a PALSAR image dated January 2010 (for the L-Band) and AIRSAR data dated July 1991 (for the P-band).

On this data, no crevasse was visible.

An estimation of the electromagnetic wave attenuation and depth of penetration in the ice sheet was also necessary. A survey of the literature was performed.

ONERA concluded that fresh snow (which was covering the lost hub fragments) should correspond to a penetration depth of around 4m two-ways with the X-band and much more with the L and P-bands. Snow falls are expected to be around 2m thick, so ONERA expected to see the hub fragments through the fresh snow layer. Underneath, due to the percolation, the layers would have a strong backscatter and act as inhomogeneities, increasing the loss of wave propagation.

The hypothesis made is that the lost hub fragments lay above this ice layer formed during the summer before the accident.

Detection tests under the snow were nevertheless discussed late 2017. The detection test of the fan hub in Nimes-Garons was an opportunistic campaign, and occurred in Nov-Dec. 2017. If any airborne search was to happen in winter/spring 2018, i.e. before the snow starts to become too "*wet*" (from May), there was no more time for any more flight tests due to aircraft availability and logistical reasons.

Moreover, if flight tests had to be performed to estimate snow penetration, the exact same snow characteristics as those on the ice sheet would be required for the tests to be reliable.

ONERA was quite confident that the radar would penetrate snow at a sufficient depth to detect the fan hub fragments. Therefore, no snow penetration flight tests were performed.

3.3.3 Recovering the parts

It was estimated that there were reasonable chances that an ONERA airborne search campaign performed at the end of the winter or beginning of spring would make it possible to locate the fan hub fragments under the snow on the ice sheet.

If this operation was successful, the way of recovering the parts had then to be discussed.

Shortly after the event, GEUS was asked to make a proposition for a ground search operation consisting in blind scanning of the computed priority zones in the search area, during a spring campaign of four weeks.

Because of the weather conditions on the ice sheet, it was out of the question to send anyone there for a long stay during the winter (until end of March). Even for a short stay, the investigation team was not able to find anyone that would be authorized or that would accept to work in such extreme cold temperatures.

Blind scanning several square kilometers in that area, with the potential presence of crevasses, is time-consuming work with limited chances of success.

An airborne operation carried out first could improve significantly the chances of recovering the parts, if located.

The decision to set up a GEUS ground recovery operation following the airborne search was made early January 2018 as it seemed to give the best chances of success.

Even if parts were located during the airborne search, it was necessary to set-up a ground recovery phase. If parts were not located during the airborne search, the ground phase would be converted into a blind search in the priority areas.

3.3.4 Search area in case airborne search is unsuccessful

As far as the airborne operation is concerned, the swath of the SAR (3 to 6 km depending on the radar parameters and flying altitudes as presented in paragraph 3.2.5) is so large that it was not necessary to restrain the search area. However, the investigation team had to consider the fact that even if all precautionary measures were taken, there was a possibility that airborne operations would be unsuccessful, meaning that no potential target would be provided to GEUS for the field campaign.

In this unfortunate case, a reduction in the size of the search area was requested.

The primary areas were defined as being the overlapping between the NTSB and Ariane computations (Fig. 43). The secondary search area was defined as the area between the two previous ones, the overlapping secondary NTSB search area and Ariane computation (Fig. 44).

The tertiary search area was an enlargement that encompasses the total NTSB search areas and most of the Ariane computation results (see Fig. 45).

The coordinates of the area corners are given in Table 4:

Primary		**Secondary**	**Tertiary**
Dark blue	*Dark red*	*Orange*	*Light green*
61.745422° -46.879801° 61.742268° -46.876823° 61.746599° -46.851589° 61.749263° -46.854593°	61.735346° -46.868874° 61.732873° -46.864770° 61.742179° -46.840839° 61.744385° -46.845679°	61.742268° -46.876823° 61.735346° -46.868874° 61.744385° -46.845679° 61.746599° -46.851589°	61.743276° -46.905362° 61.725735° -46.878229° 61.741007° -46.830514° 61.753678° -46.842806°

Table 4: search area coordinates for ground campaign in case Air search campaign is unsuccessful

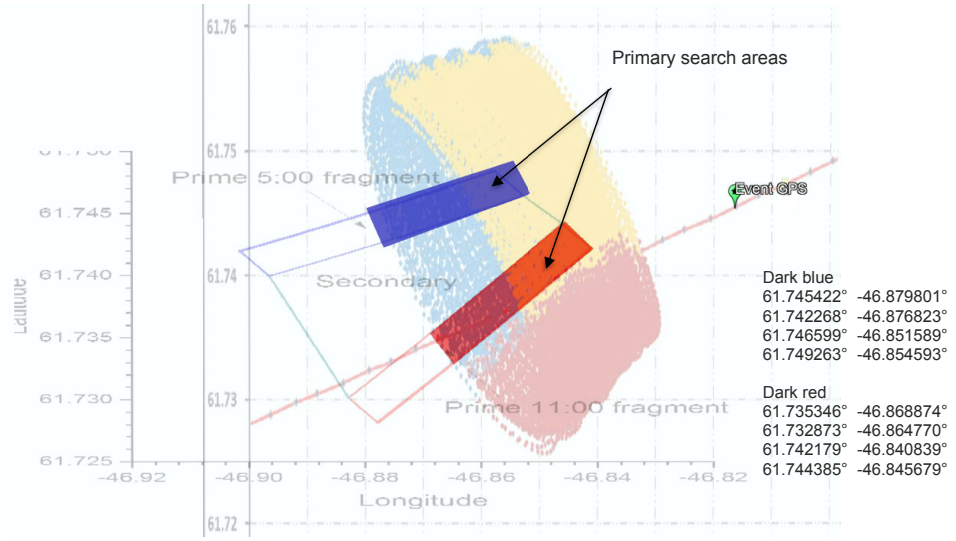

Fig. 43: primary search areas (dark blue and dark red, 0.5 km2 each), defined end of March 2018 in case airborne search is unsuccessful

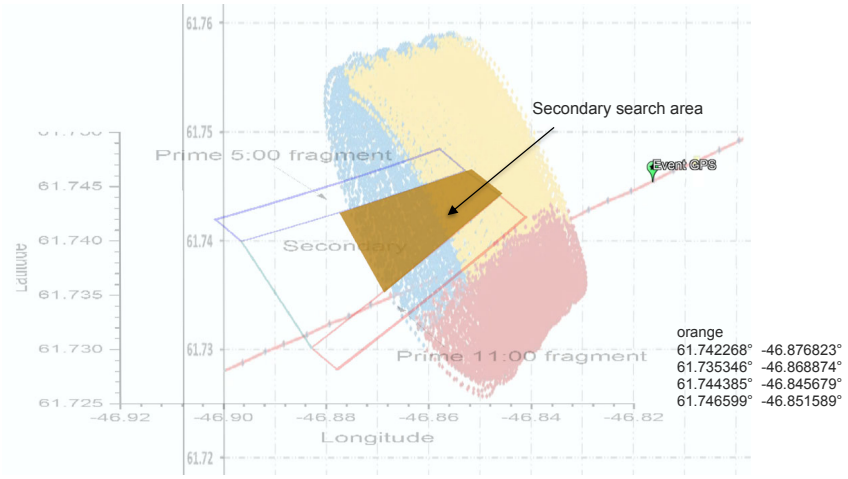

Fig. 44: secondary search area (orange, 0.93 km²), defined end of March 2018 in case airborne search is unsuccessful

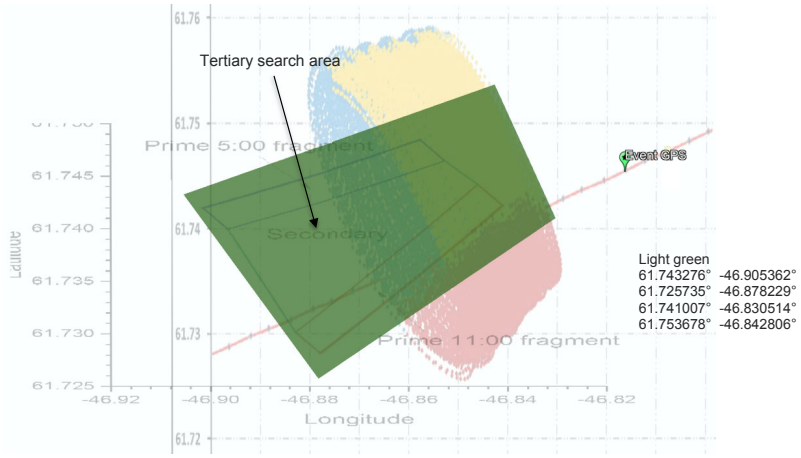

Fig. 45: tertiary search area (light green, 6.35 km²), defined end of March 2018 in case airborne search is unsuccessful

3.4 GREENSAR Operation

3.4.1 Preparation

The BEA initially asked ONERA to organize the search operation in Greenland during the winter of 2018. ONERA proposed three radars components in X (9.5 GHz), L (1.3 GHz) and UHF (340 MHz) bands in a full polarimetric configuration. The objective was to take advantage of the penetration under snow capabilities of the lower frequencies in particular with the UHF band.

The measurement flights had to take place between February and April 2018 in order to benefit from the state of the snow during the coldest period when the snow is ''*dry*'' which is favorable for the penetration effect. However, it was also a compromise with weather conditions, as the later in the year, the warmer the temperature, the better the weather, and the longer the daylight.

The mission was thus planned for the beginning of April 2018.

For calibration purposes, ONERA asked if calibration items could be buried in the search area. ONERA generally uses two kinds of reflectors: a corner reflector (or trihedral) and a Luneburg sphere (Fig. 46).

GEUS proposed to bury these items during a short reconnaissance mission, shortly before the measurement period in order to limit the shift of the targets due to ice sheet movements (Fig. 47). A test hub fragment (made from a 93% scale part, see Fig. 48) was provided by EA and was also buried on site, as a reference, as its GPS location was known.

This mission occurred on March 24, 2018.

Fig. 46: trihedral and sphere in their transport crate

For calibration purposes, the reflector was buried with its leading lip parallel to 256.5° and opening toward 166.5°, which correspond to "*true north*" values of 233° and 143° respectively, as in this location, the deviation between true north and magnetic north reaches 23.5°.

GEUS took the initiative of creating an ice lens in order to check what its backscatter would be on the radar images. This was done by burying a sledge full of melted water.

The final position of the reflectors and reference objects (one Luneburg sphere, one corner reflector, one test hub, one ice lens and one empty hole) are shown in Fig. 49.

Fig. 47: GEUS member burying Luneburg sphere on ice sheet

Fig. 48: part of a fan hub mock-up on its sledge, later referenced as “test hub” (left picture), and once buried (right picture)

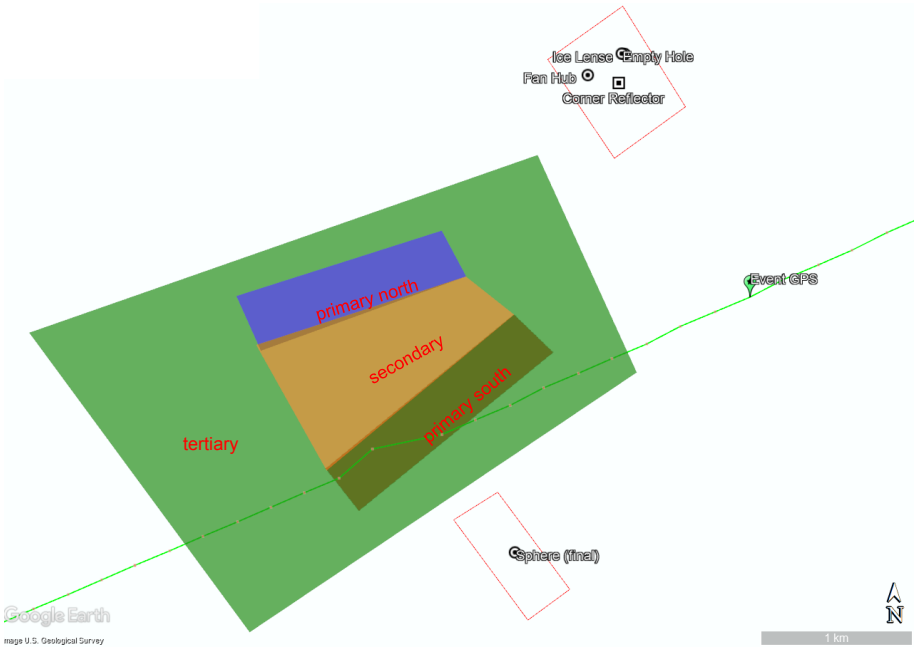

Fig. 49: position of reflectors and references items compared to search area (in red, defined in paragraph 3.3.4)

Local facilities for aircraft and staff led the team to consider Kangerlussuaq (with a runway of 2810 m) as the primary base, and Narsarsuaq (with a runway of 1830 m) as the secondary (Fig. 50). Measurements would be made from these two airports over the search zone on which the F-HPJE parts were supposed to lie.

Due to the limited flight time dedicated to measurements (for safety, the plane must keep a reserve of fuel to land on one or the other of these airports) ONERA proposed the acquisition of between 5 and 8 measurement lines per flight, as the autonomy of the aircraft is around 2.5 hours.

The onsite team consisted of one attendee from the BEA, one from AIRBUS, one from the NTSB, two pilots (captain and first officer) and one mechanic from AVDEF, as well as nine members from ONERA: five radar operators, two experts in data processing and two project managers. The chief of operations from AVDEF was also present for three days.

The ONERA and investigation team were installed from April 3 to April 19, 2018 in Kangerlussuaq Airport, with data processing equipment conveyed from France, in order to produce quick look images after each flight.

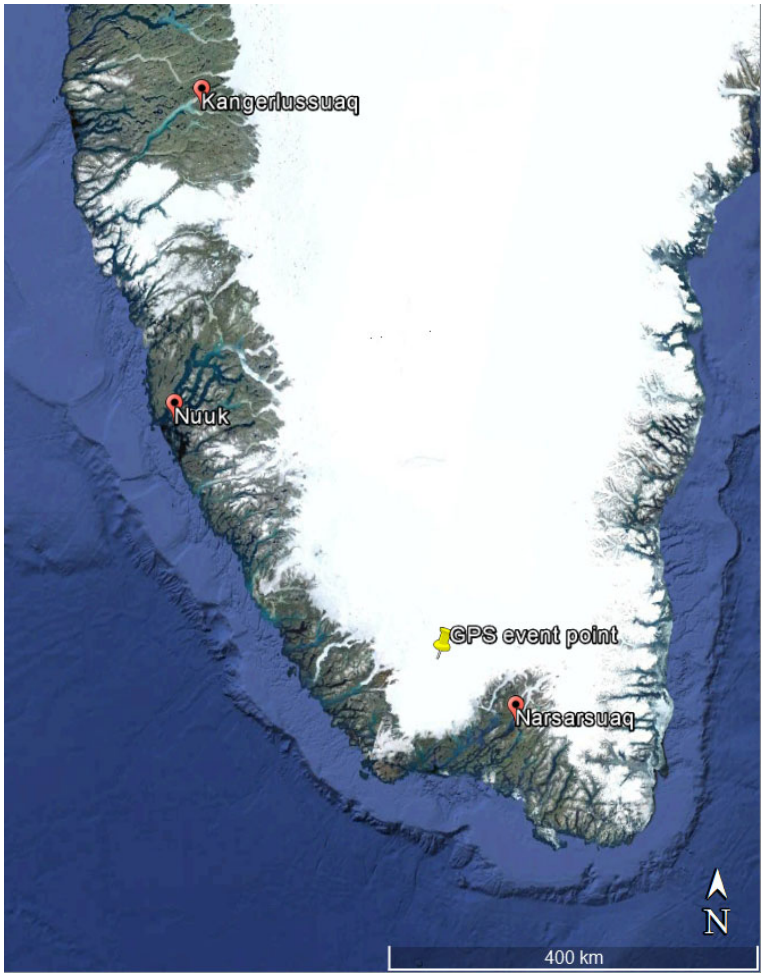

Fig. 50: event point compared to Kangerlussuaq and Narsarsuaq locations –
Nuuk is the capital and largest city of Greenland, but its airport runway is only 950 m long

3.4.2 Validation flight (April 5, 2018)

The objectives of the validation flight were to validate that all the hardware and software was working as expected, to optimize the post-processing parameters and to determine what the electronic delays of the system were.

For this purpose, a second trihedral (a first trihedral was already buried under the snow on the search area) was accurately positioned on Kangerlussuaq Golf course (67°01'27.14729»N 52°38'1.29678»W), aligned with 062° (Fig. 51).

Fig. 51: trihedral position

The validation flight was performed on April 5. During the flight, two scans with the X band and two scans with the L and UHF bands were performed over the trihedral location ("*Kangerlussuaq area*"). Then, two other scans were performed over an area with characteristics which were deemed similar to those of the ice sheet near the search area. It was located 100 Nm east of Kangerlussuaq and required 20 minutes of flight time from the golf course. The first pass was dedicated to the L and UHF bands and the second pass to the X band.

Data post-processing started immediately after the flight. Electronic delays were measured and processing parameters were refined. Radar images of the areas were produced, as shown in Fig. 52. On this picture, the trihedral (red circle) could be clearly detected. It was also possible to see the ground features underneath the snow, demonstrating that snow was well penetrated by the X band.

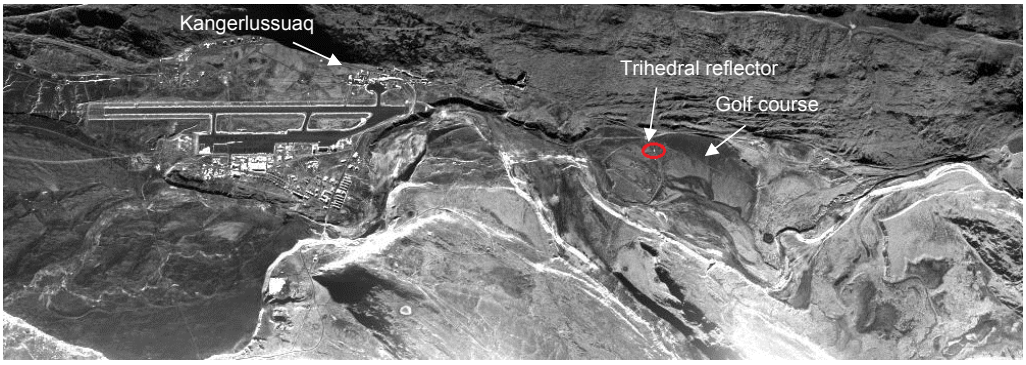

Fig. 52: X-band radar imagery of Kangerlussuaq area

Post-processing activities were continued for accurate calibration of the system and post-processing parameter refinement.

3.4.3 First set of measurement flights (April 6 to 8, 2018)

The objectives of the first set of search flights was to accomplish several predefined measurement passes over the search area. Given the weather conditions in Narsarsuaq (UAK) which were quite limiting for the aircraft equipped with its two SETHI pods, the following flights were performed:

- Kangerlussuaq (SFJ) – Narsarsuaq (UAK): X band measurements, three passes heading 233° and three passes heading 053°;
- UAK – SFJ: UHF (P) and L band measurements, three passes (heading 233°, 53° and 323°).

The outbound flight (SFJ-UAK) dedicated to the X band measurements was performed on April 6.

The measurement passes are shown in Fig. 53. Radar coverage for these passes is shown in Fig. 54.

Due to weather conditions, the crew was not able to take off from UAK the same day. The next slot where conditions were acceptable was on April 8 (two days later), end of morning. It was decided to take no risk doing a local UAK-UAK flight which would have collected more data, but instead to fly directly to SFJ, in order to get data as soon as possible and not have the aircraft blocked in UAK again. The return flight was performed on April 8, with L and UHF (P) band measurements.

The measurement passes are shown in Fig. 55. Radar coverage for these passes is shown in Fig. 56.

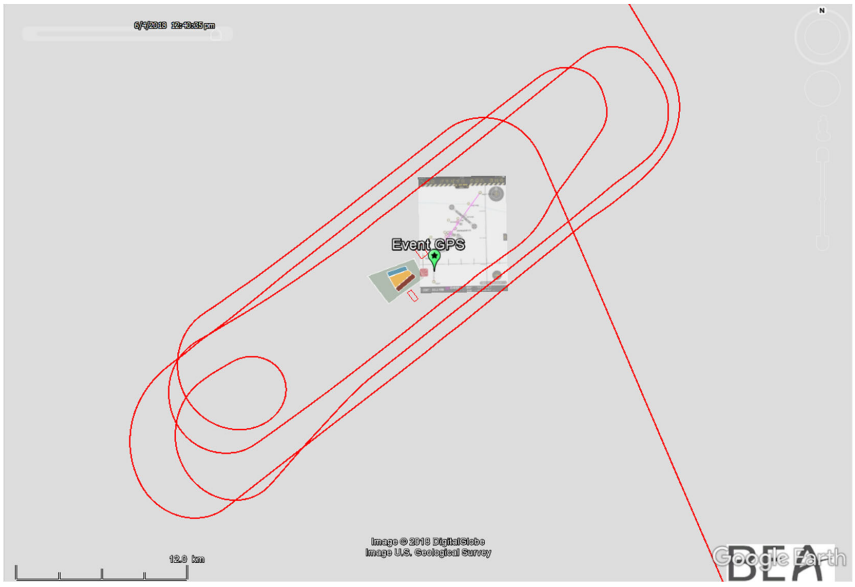

Fig. 53: X-band measurement passes – aircraft trajectory (outbound flight)

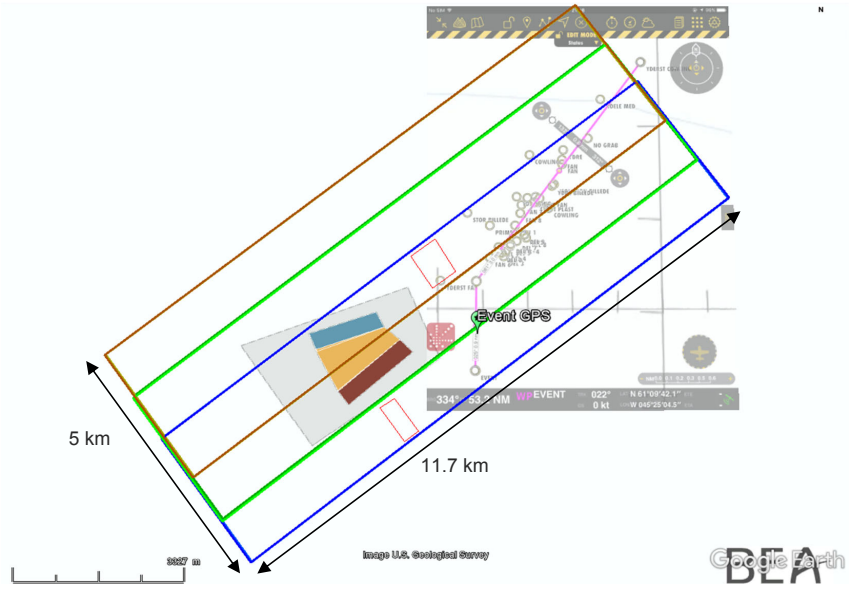

Fig. 54: X-band coverage of the six measurement passes (outbound flight)

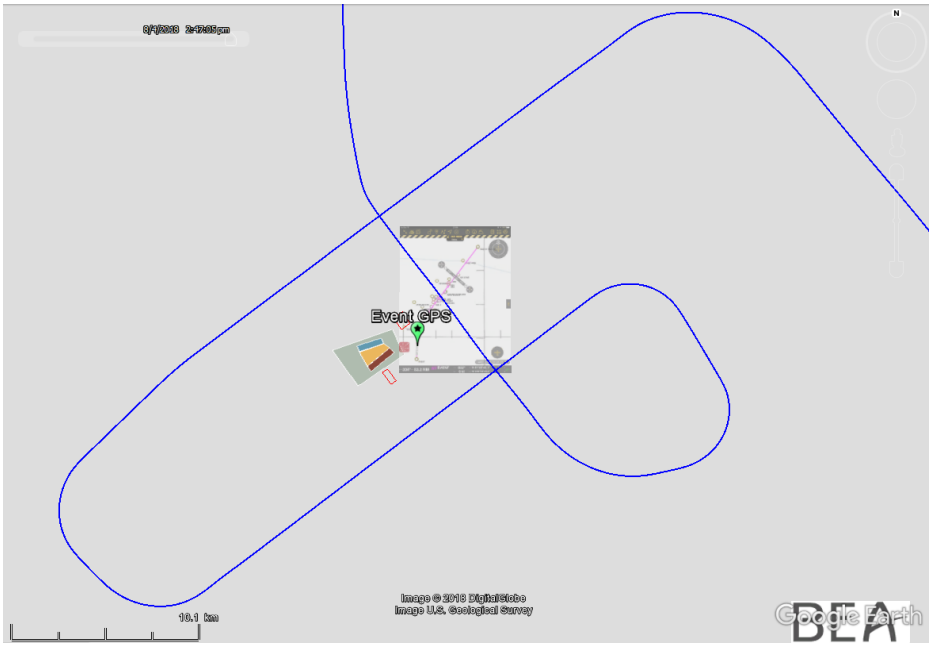

Fig. 55: L and UHF (P) band measurement passes – aircraft trajectory (return flight)

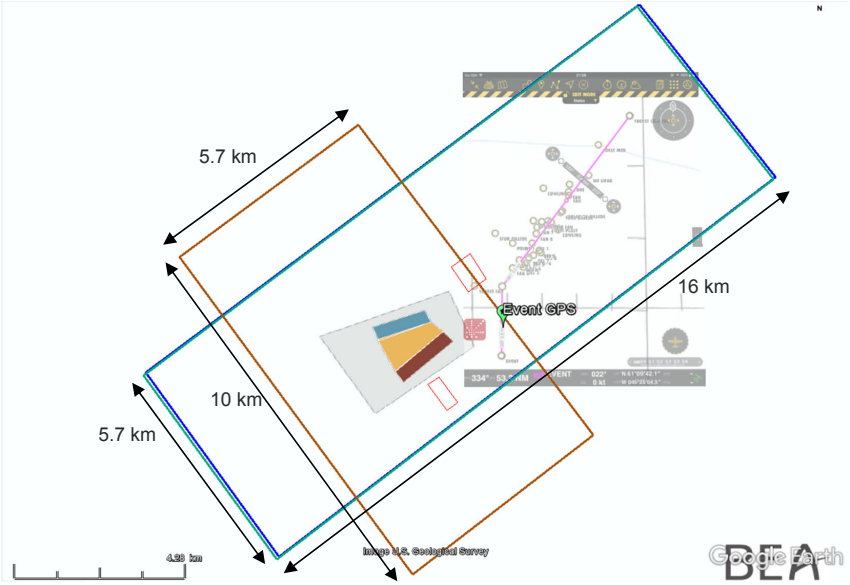

Fig. 56: L and UHF (P) band coverage of the three measurement passes (return flight)

The post-processing of data showed the following:

- As first results, the trihedral could be detected with the X band. The sphere was detected with the UHF (P) and X bands. The test hub could not be detected at that time, either with the X, L or UHF(P) bands.
- Several filters were tried with no real improvement. The images were analyzed visually (for information, a P band image is 1.6 GB (11630 x 18229 pixels), a L band image is 1.3 GB (9000 x 18711 px), and an X band image is 13 GB (22135 x 76000 px).
- The search area lay over a field of crevasses, clearly seen with the L and UHF (P) bands, and barely seen with the X band (see Fig. 57). An analysis over the crevasses indicated that the UHF (P) band could penetrate at least 15 m within the ice sheet/snow cover, the L band at least 3 and 5 m and the X band was believed to detect the surface only (or penetrate some surface snow).
- Several "*candidates*" were identified. The work then consisted in distinguishing false and true candidates, looking at the whole images, and gaining robustness in the detection process.

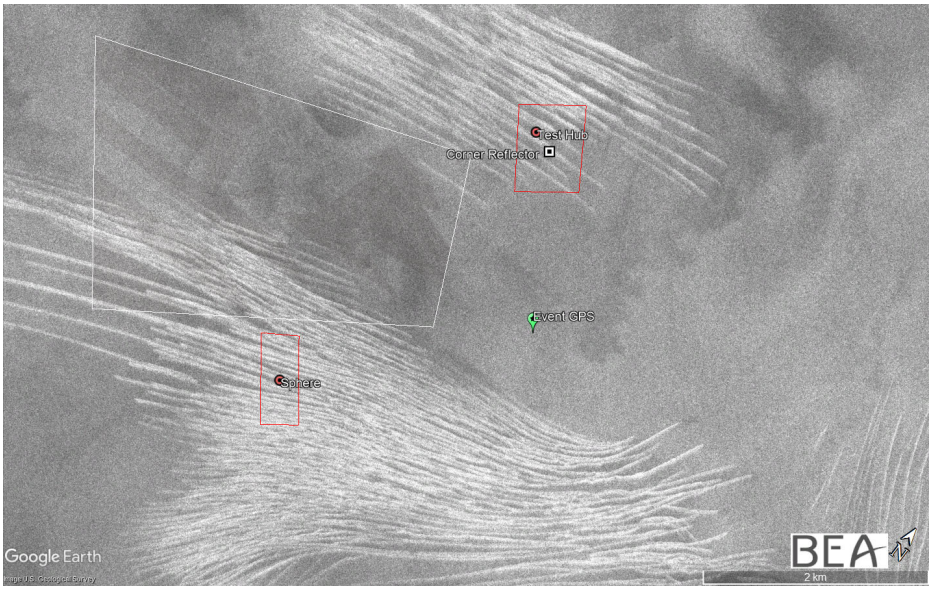

Fig. 57: search area with crevasses seen with P band

3.4.4 Second set of measurement flights (April 10 to 11, 2018)

The main objective of the second set of search flights was to perform the measurement passes over the search area which had not yet been performed, in order to complete the set of recorded data.

In order to have a better detection probability within the crevasses, the radar was reconfigured with a depression angle of 50° instead of 40° for the L band. The UHF(P) band remained configured with a depression angle of 45°.

The first flight of this second set was performed on April 10 with UHF(P) and L band measurements. The aircraft trajectory is shown in Fig. 58. The corresponding radar coverage is shown in Fig. 59. Due to weather, the aircraft was not able to take-off again on the same day as the first flight. The next flight was performed the day after, on April 11, in the morning. Weather conditions permitted a local flight (Fig. 60) and acquisition of the six missing X band passes (Fig. 61). The aircraft landed at UAK again.

Finally, the aircraft took off again from UAK on the same day for the return flight to SFJ, just before the weather degraded rapidly (Fig. 62). This third flight of the set was dedicated to calibration with the 50° radar depression angle. Passes were performed over the trihedral again, disposed on the golf course for that purpose. The calibration flight path is shown in Fig. 63.

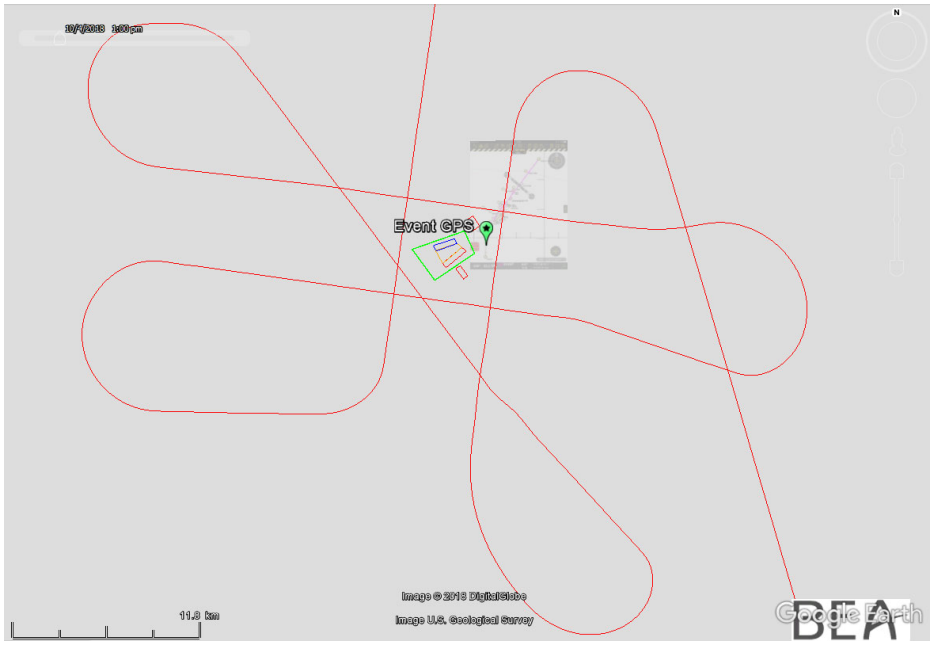

Fig. 58: first flight of set (SFJ-UAK): five passes with UHF(P) and L band

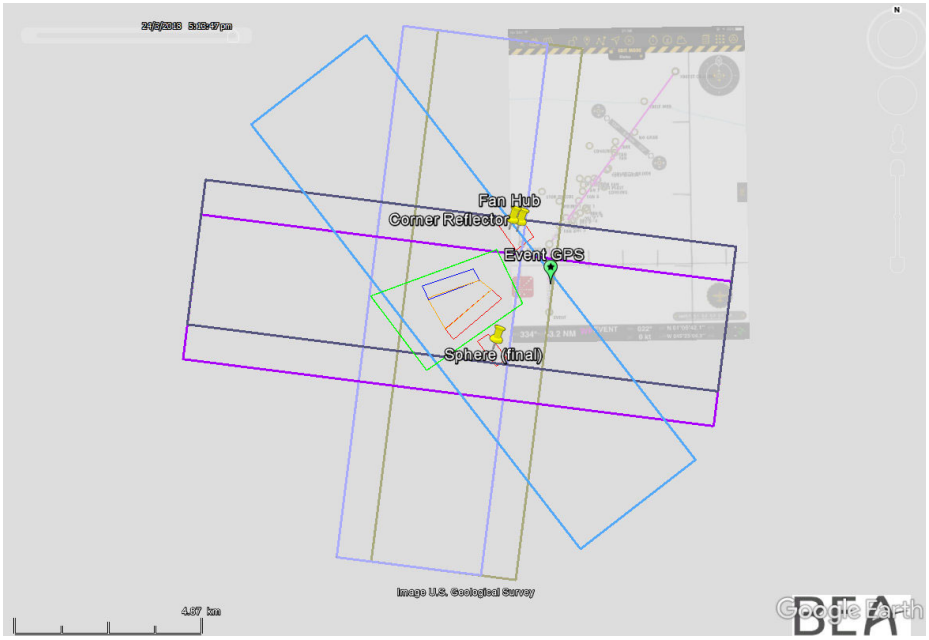

Fig. 59: UHF(P) and L band coverage, second set of flights

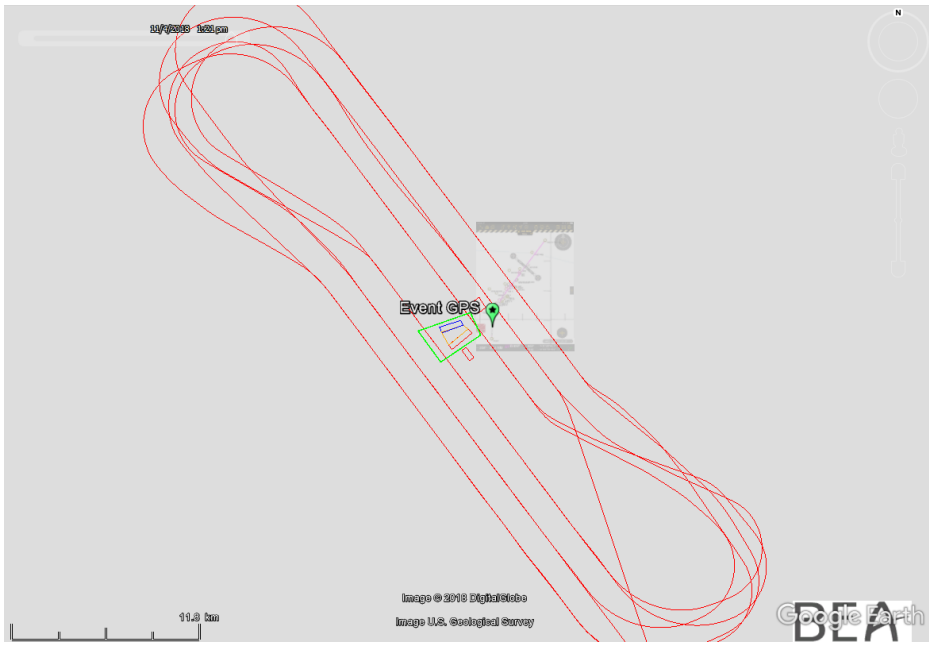

Fig. 60: second flight of set (UAK-UAK), six passes in with X band – aircraft trajectory

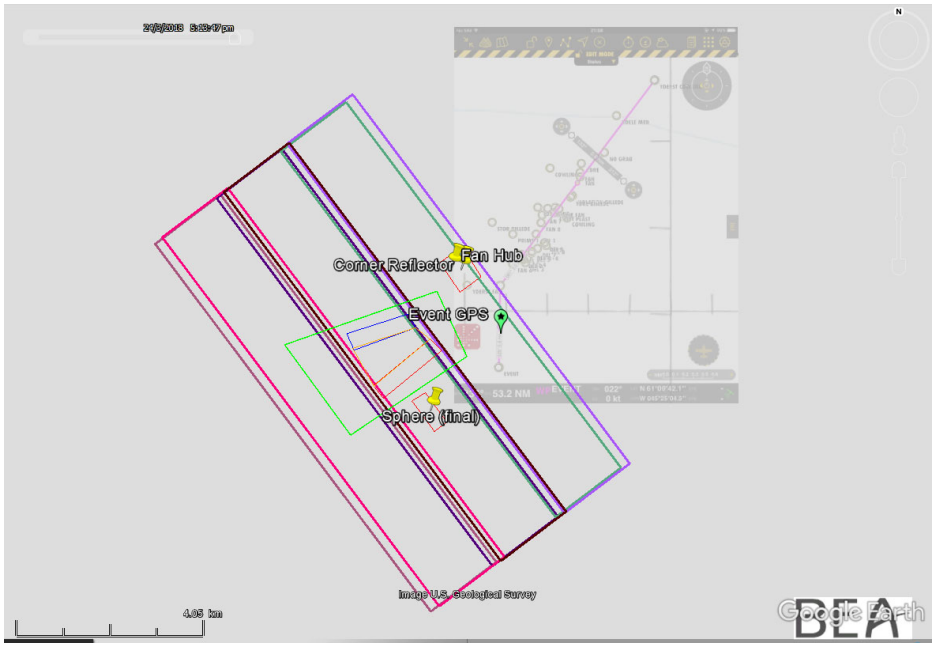

Fig. 61: X-band coverage, second flight of set

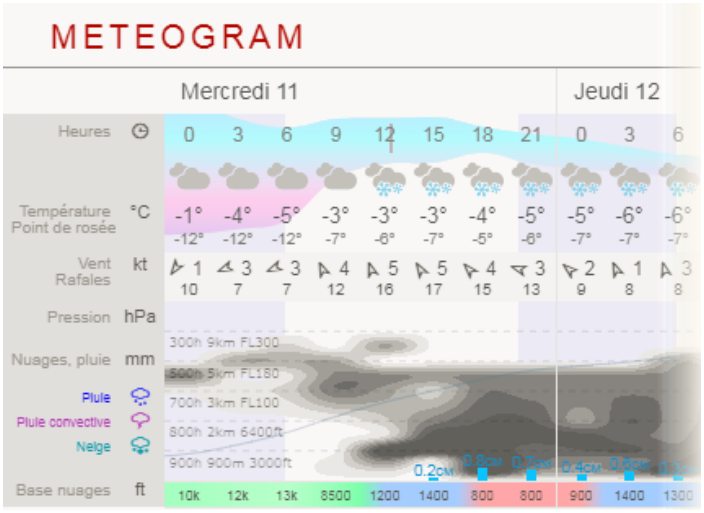

Fig. 62 : weather forecast for April 11, updated on same day in morning

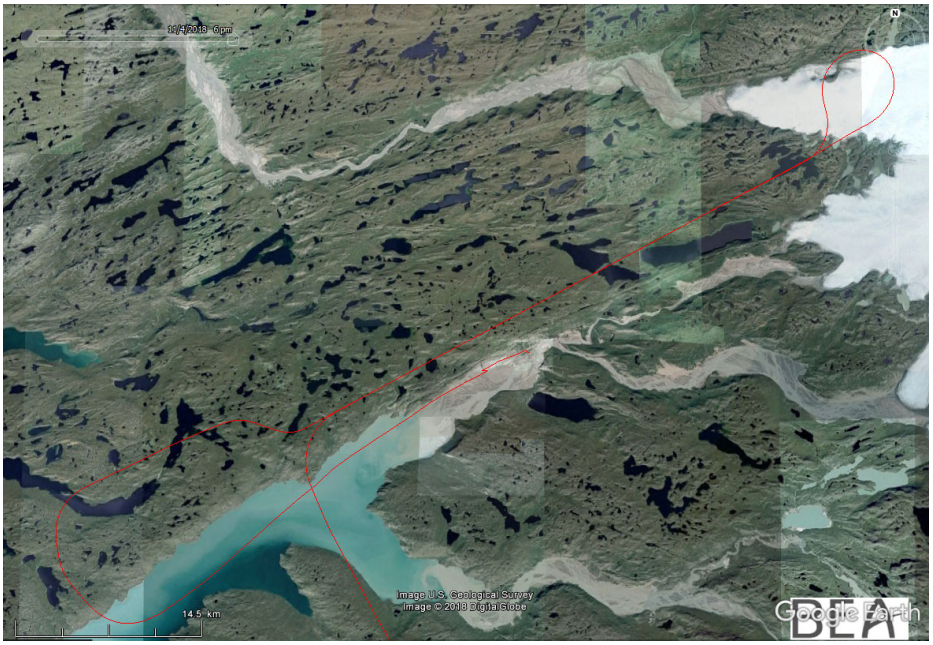

Fig. 63: third flight of set, calibration over Kangerlussuaq

Post-processing of the data started immediately after the aircraft landed and the recorders were downloaded.

After the second set of flights, ONERA stated the following:

- X band radar did not penetrate snow as much as expected (even if the snow penetration during the validation flight was ok) – it has been suggested that the X band performance over the search area was due to the snow's characteristics.
- P and L band radars penetrated into the ice sheet and detected crevasses in the search area.
- The background scatter noise on the images prevented the automatic search algorithms from detecting targets, as the contrast ratio was not high enough.
- X band detected the trihedral and the sphere.
- L and P band detected the sphere.
- The test hub was still being looked at with the second flight's set of data.

Due to the large number of crevasses in the field and higher than expected background scatter noise, various algorithms were created to eliminate unreliable detections and focus on potential targets. Depth was selected as a search criteria (targets below 10 m were no longer considered). Images with a scan direction parallel to the crevasses were preferentially analysed to help provide targets not linked to crevasse features.

Several areas of interest were identified but still further processing and analysis to verify feasibility was needed.

3.4.5 Third set of measurement flights (April 14, 2018)

The main objective of the third and last set of flights was to perform interferometric[15] radar scan passes over the area to obtain height information for the detected targets using another technique, and to explore if height can be used as a discriminant for detection (ice layers will have a lower altitude than the pixel containing the hub).

With this in mind, it was decided to perform UHF(P) and L band measurement passes with the following headings: 008°, 143° and 323°. The radar was reconfigured to a depression angle of 40° for the L band and the UHF(P) band remained configured with a depression angle of 45°. The altitude was changed between passes at the same heading to allow the interferometric analysis (first pass altitude was 18100 ft, second pass was at 17100 ft and third pass was at 17940 ft).

The outbound flight trajectory (Kangerlussuak – search zone - Narsarsuaq) is shown in red in Fig. 64 and Fig. 65. Fig. 65 also shows the radar coverage for this flight.

[15] Interferometry is a family of techniques in which waves are superimposed causing the phenomenon of interference in order to extract information.

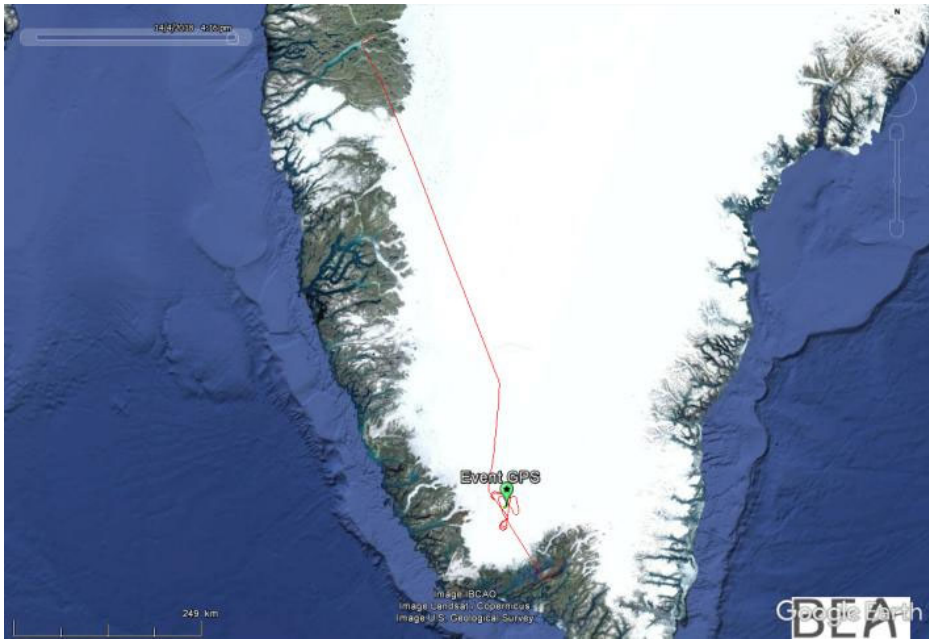

Fig. 64: first flight trajectory for interferometric measurements

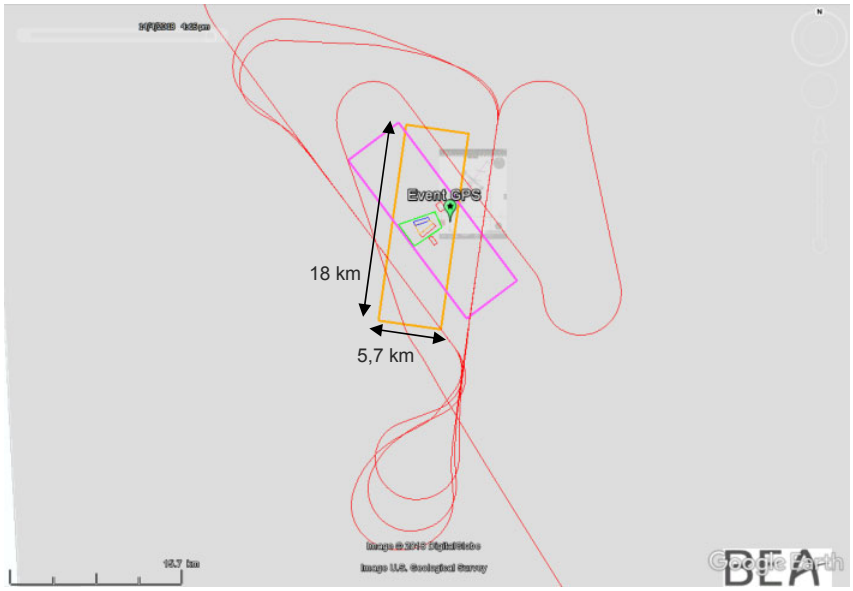

Fig. 65: UHF(P) and L band coverage and first flight trajectory for interferometric measurements

The return flight (Narsarsuaq – search zone – Kangerlussuaq) was performed the same day. The trajectories and radar coverage are presented in Fig. 66 & Fig. 67.

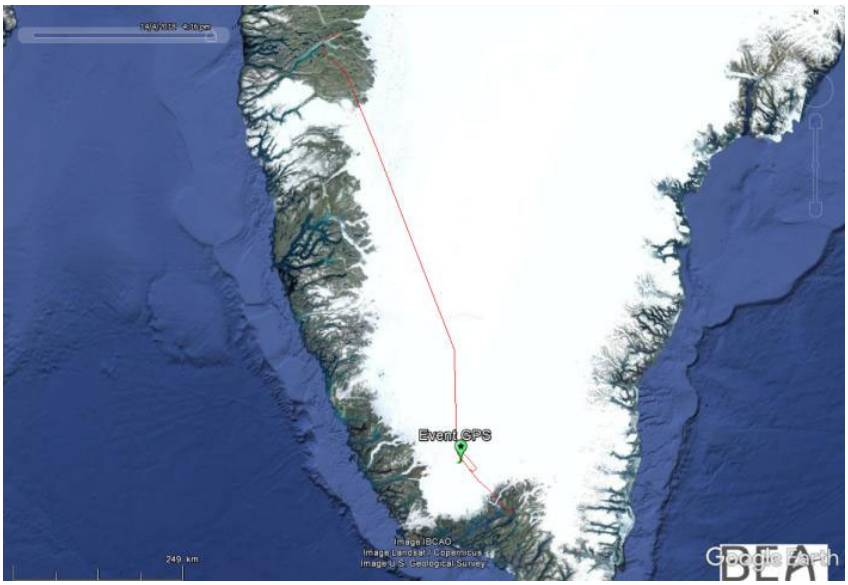

Fig. 66: second flight trajectory for interferometric measurements

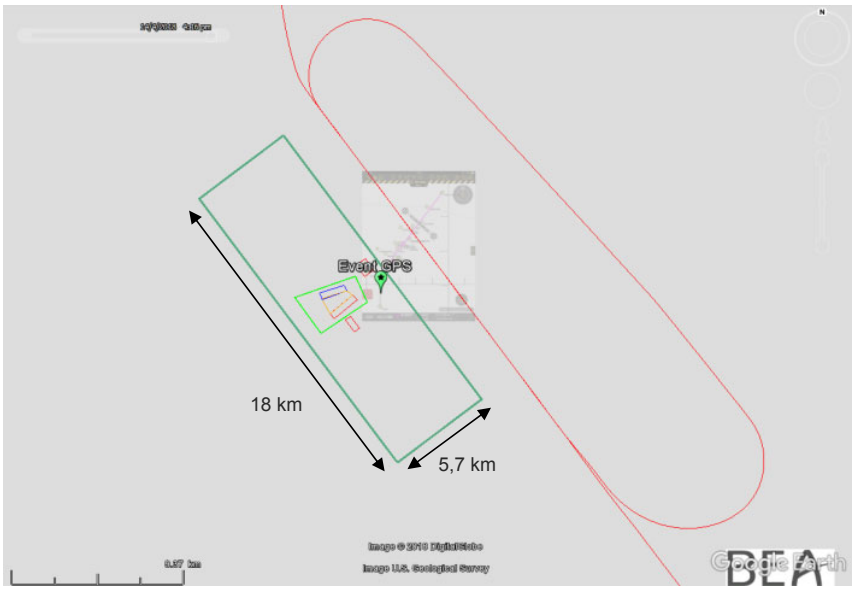

Fig. 67: UHF(P) and L band coverage and second flight trajectory for interferometric measurements

Fig. 68: Avdef Falcon 20 equipped with its two radar pods, back at Kangerlussuaq Airport

The post-processing of data started immediately after the aircraft landed and the recorders were downloaded. After the N° 2 set of flights, 11 points were considered as potential targets. They were the ones that were common to all three polarization images at different headings, common to P & L radar bands and less than 10 m deep, but none was located in the predefined search area.

As a hub fragment may not reflect radar waves on all headings, being only part of a hub, ONERA was requested to re-run the analysis, looking for common points in 2 out of 3 polarization images only, instead of common to all 3 images as previously.

With this new criterion, new targets were identified within the search area, but refinement and confirmation of the relevance of these targets was still being analyzed in the following days with advanced processing techniques (Fig. 69).

After the three sets of flights, the pods were removed from the aircraft for its return flight to France. Post-processing and data analysis were continued before and during the ground search operation carried out by the GEUS team (see next chapter) in order to provide them with updates if necessary.

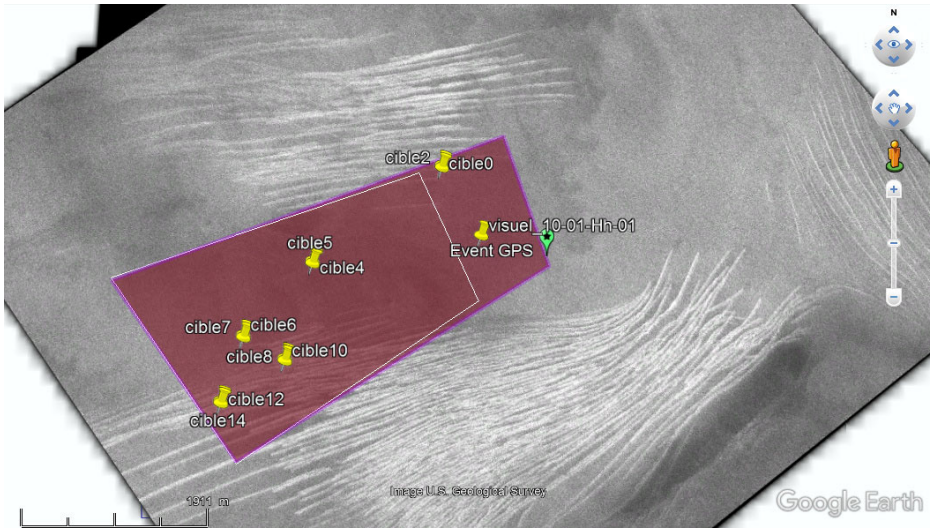

Fig. 69: potential points within search area, further analyzed for confirmation and relevance

3.5 CAMP RECOVERY

3.5.1 Introduction

The objective of the GEUS field campaign was to reach the ONERA targets, confirm the detection with a GPR, dig a hole at the detection location to determine what laid underneath the snow if the detection was confirmed by the GPR, and if a fan hub fragment was discovered, recover it and take it back to Narsarsuaq Airport.

If no ONERA detection was confirmed to be a piece of debris, the back-up plan was to carry out a blind search with the GPR, over the entire search area, looking at priority areas first, then secondary and tertiary areas, as defined in paragraph 3.3.4.

The final ONERA approach for target determination was to consider targets which:

- responded at P and L Bands and were not too directive (signing at two headings at least);
- were within a depth of 10 m compared to the ICESAT Digital Elevation Model[16].

The GPS coordinates of ONERA's most consistent targets thus obtained were the following:

NAME	LAT	LONG
Target_01	61.745517°	-46.880175°
Target_02	61.744321°	-46.871506°
Target_03	61.744267°	-46.871818°
Target_04	61.735043°	-46.868160°
Target_05	61.746310°	-46.830680°
Target_06	61.764459°	-46.818955

Fig. 70 shows the target locations as well as the search areas for the blind search.

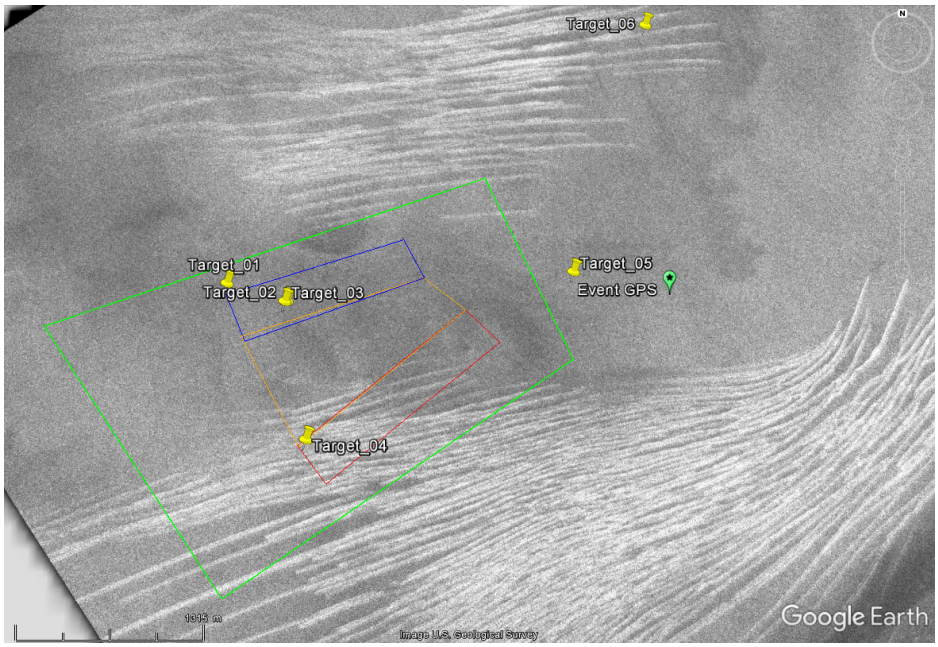

Fig. 70: targets identified by ONERA, given to GEUS team.
The background image is a radar image provided by ONERA from the measurement campaign showing clear crevasse fields

The target coordinates were given to GEUS. According to ONERA, a 5 m-radius circle had to be considered as a measurement uncertainty.

The agreed timeline for the field campaign was as follows:

- 1. Formal identification of the test hub with the available means of detection (GPR).
- 2. Check of Target_01 to 03 as first priority (assuming that the test hub GPR scan was already performed and was positive...).
- 3. Check of Target_04, if safety assessment was favorable, as this target appeared to be over a crevasse field.

[16] ICESAT Digital Elevation Model (DEM) is a model of terrain elevation that was used by ONERA to compute the depth of the targets under the surface (refer to https://nsidc.org/data/nsidc-0305 and to (DiMarzio, 2007) for further information).

- 4. Blind search of the first two priority areas (blue and red rectangles) - for the red rectangle, GEUS was asked to rely on their safety assessment for its scanning (if entire area was permitted or part of it only).
- 5. Scanning of the second priority area (orange) (same principle as red rectangle regarding safety).
- 6. Check of Target_05.
- 7. If nothing found so far, completion of the scan of the third priority area.
- 8. If time was remaining, check of target_06 (with same concern about safety).

ONERA provided GEUS with a GEOTIFF file of the scanned terrain, providing the location of crevasse fields. This file helped GEUS to carry out their safety assessment.

A back office was set-up in Narsarsuaq, South Greenland, starting from April 24. The team consisted of two safety investigators from the BEA (including one metallurgist), one safety investigator from the NTSB, one safety investigator from the AIB-D, and one adviser from EA. The role of this back office was to receive, examine and manage recovered parts, if any, and advise or redirect the field campaign when necessary.

Almost every day, when possible (communication was sometime difficult from this remote area), GEUS issued a field report to the AIB-D, which was forwarded to the back office in Narsarsuaq. A summary of the field campaign and back office activities is presented in the following chapter.

3.5.2 Progress of the mission

The first GEUS team members landed in Narsarsuaq on April 17, 2018. The first three days were dedicated to logistics: meeting with helicopter pilots, equipment packing (propane bottles, fuel, snowmobiles, generators, personal and scientific equipment, food) and sling loading.

Two sling loads were positioned on the ice sheet by helicopter on April 19.

A Norlandair Twin Otter was loaded the same day with 250 kg of cargo and one snowmobile. The day after, it transported two passengers and the cargo to the ice sheet. The plane returned to Narsarsuaq where it was reloaded with one more snowmobile, 300 kg of cargo and two other passengers. After one more return, the rest of the cargo and the last two passengers were transported from Narsarsuaq to the site. All cargo and 6 pax were on the ice sheet on April 20, 1 pm. The team set up a kitchen tent, a toilet tent, a science tent, the personal sleeping tents, organised the cargo, moved the fuel away from the camp, established a cargo line, and set up the polar bear trip wire around the sleeping quarters. Fig. 71 gives a good view of the camp.

The next day (April 21), the generator was turned on and the radar batteries were charged. Safety in camp was improved: the team tested the rifles, set up flaglines for orientation in case of a white out, and established a polar bear trip wire around the kitchen and science tents.

A 3.1 m snow pit was dug to get an accurate density measurement of the snow which was needed for calculating the depth of the radar signals (Fig. 72). The radar was powered up and tested around the camp.

On April 22, tests of the radar were going on, data from the day before and density measurements were analysed. Four persons went out to one of the crevasse fields identified by the airborne radar. Using ropes, one person safely traversed a crevasse with the radar. Back in camp, the analysis of the data did not reveal any sign of crevasses in the top 60 m, meaning that they were probably filled in with snow. A sledge for dragging the radars after the snowmobile was then constructed.

To prevent snow drifting into the tents, snow walls were built around the tents.

Fig. 71: recovery camp – sleeping tent (foreground), science and kitchen tents (background) – flags are used for orientation in case of white out (photo credit: GEUS)

Fig. 72: snow samples for density measurement (photo credit: GEUS)

On April 23, the generator stopped providing electricity. Fortunately a spare one was available. Despite several attempts to repair it, the team had to order a replacement from Copenhagen.

In the afternoon, ONERA target N° 5 was checked. This was the closest target to the camp, and GEUS thought it was a good opportunity to test the radar sledge, the construction of which had been finished in the morning. They drove a dense 20 m by 20 m grid with 1 m spacing but found no obvious reflections that prompted further investigations. To help calculate depth, they dug another snow pit and cored down to 5.2 m to get detailed snow density. They saw several very thick ice lenses. Afterwards, two of them drove to the crevasse field nearby where the test hub was buried and crossed several crevasses. They did see some buried crevasses at 40 m but not where the airborne radar scan indicated they would be (due to radar geometry, a difference in altitude results in a seeming difference in localization).

Based on this survey, they decided that it was safe enough to drive out and retrieve the buried fan hub and the corner reflector. The corner reflector was too close to the surface to show on the radar but the test fan hub was visible (Fig. 73). It seemed that the radar antenna should ideally be within one meter of the fan hub for the signal to be very clear so survey plans had to be revised for the radar grids to be denser. Initial passes were 5m in width. Based on the test hub results, the swath was determined to be too large for confident detection. The width of the detection passes was reduced to 2 m and finally 1 m.

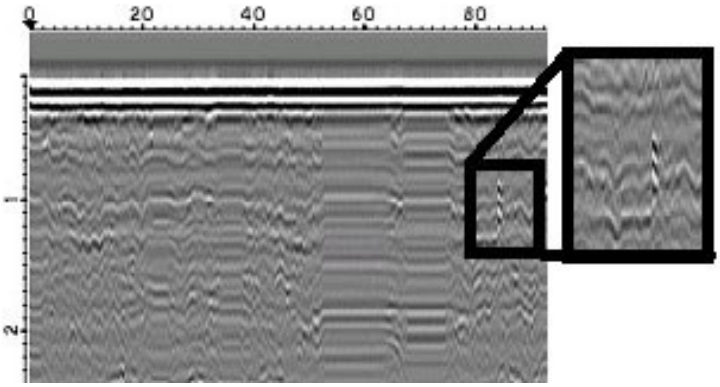

Fig. 73: test hub signature on GPR imagery

On April 25, a team checked target sites N° 1 and 2. No detection was obtained with the GPR. The team decided to check whether the radar settings were optimised and buried the test hub again at a depth of approx. 2.5 m, as a test point. They drove across the burial site several times and most of the times they were able to identify a signal. Unfortunately, they also had some false positives and therefore decided to continue to optimise the detection procedures.

After many different approaches, they decided that the 250 MHz antenna provided the most consistent results.

The day after, they went back to targets 1, 2 and 3 and carried out a dense grid with the 250 MHz antenna.

In order to better understand the data provided by ONERA, they investigated the snow properties further by drilling a 11 m core. They saw very thick ice lenses, some up to 60 cm thick, indicating substantial melting in the summer.

On April 27, the team went back to the targets N° 1, 2 and 3 locations, to look at them again with denser radar grids and different pass alignments to ensure that these three sites could definitely be ruled out. The northern priority search area was then flagged in anticipation of a systematic search (first priority blue area in Fig. 75).

In preparation for a snowstorm, the team built snow walls around all the tents and secured everything.

On April 28, the GEUS team decided to continue radar acquisition despite poor weather conditions. Two detections close to targets N° 2 and 3 were observed. Digging these two most promising reflectors, 2.5 to 3 m deep, only revealed very thick ice lenses.

At that time, given the fact that no ONERA target had been confirmed to be a piece of debris, the back office team decided to convert the ground campaign into a systematic blind search. However, also given the need for a denser radar grid than expected (see an example of dense grid scanning in Fig. 74), and given the time constraint, it was necessary to define smaller priority areas for a systematic search compared to the initial priority areas. It was clear that the initial priority areas as defined in Fig. 75 were too extensive to be completed before the end of the campaign.

Fig. 74: dense grid scanning

The probable size of hub fragments discussed in paragraph 3.1.3 and computation matching between the Ariane and NTSB calculations (refer to paragraphs 2.3 and 2.4) were considered to refine the search areas. Fig. 76 shows the new zones obtained, called Zones A, B, C and D. Zones A and B became first priority.

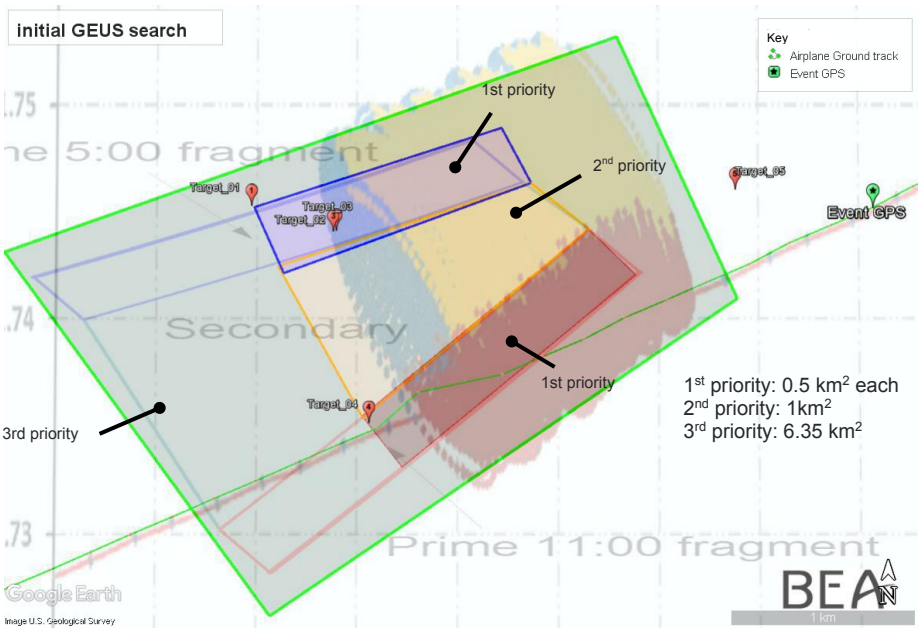

Fig. 75: initial search areas

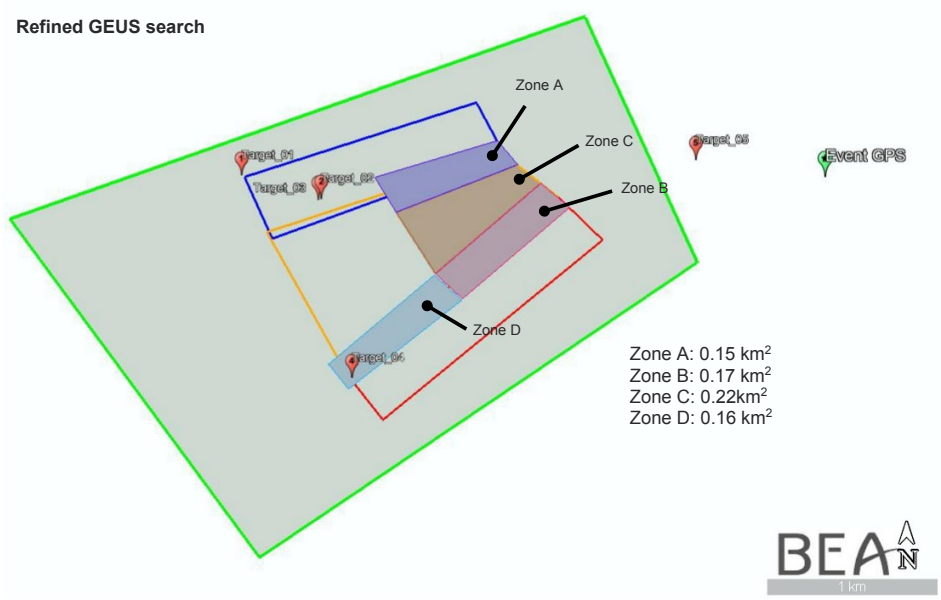

Fig. 76: refined search areas

The spare generator was finally delivered by helicopter on April 29. The back office team took advantage of this helicopter flight to provide GEUS with the updated search area coordinates. The next several days were dedicated to the dense radar grid scanning of zone A.

In parallel, the safety assessment of the southern crevasse field was started, to find out if extending the search in this region would be feasible. At a first glance, the crevasses appeared snow-filled.

On May 2, GEUS noticed that the new search areas were referenced with the October 2017 timeframe and the ice had flowed approx. 30 to 40 m since then, in a southwesterly direction. This meant that 15% of the area that had been searched in the past two days was outside the primary search area (to the north, in the previous primary search area, so it was not a total waste of time), and also that 15% of the most southern section of the newest «primary» region had not been scanned. After noticing this error, the corners of the search box were adjusted using the MEaSURes (NSIDC 0725) 2016 average annual velocity[17].

[17] https://nsidc.org/data/nsidc-0725
see§3.1.2

On May 4, two holes were dug after unusual radar features were identified, each 2.5 m deep and approximately 2 m wide. One contained a thick but localized ice lens that most probably created the interesting radar feature, and the other contained nothing of particular interest. The same day, the northern primary zone search (zone A) was completed, with no finding.

On May 7, the team did a safety assessment of the southern crevasse field. As a result, GEUS decided to not survey zone D and to cut off the southwest corner of zone B. In zone D, the crevasse field was opening and many crevasses reached to within approximatively 3 m of the surface. Their width appeared to be approximately 5 to 7 m and a lack of layering inside the crevasses meant that they might be air-filled. In the southwest corner of zone B, one large crevasse extended to within 6 m of the surface, but all layers above it showed down warping, suggesting a wide crevasse and/or a weaker snowpack above it.

One explanation could be that the southern crevasses at the upstream edge of one crevasse field were young and opening and extended to near the surface, while the northern crevasses at the downstream edge of another crevasse field were old and closing and had around 10 years (40 m) of accumulated snow on top of them. The latter were safer to work over. They all appeared to be tensional crevasses.

On May 8, the team searched zone B, except for the southwest corner with the crevasses. They started to search in the northwest corner of zone D after determining it was safe. In addition, they also began to search in zone C.

A target was identified in the data collected the day before in zone B, but looked similar to previous targets which turned out to be ice lenses. This target was dug on May 9, 2.5 m deep, 2 m wide, 6 m long, to finally find only snow and ice.

On May 9 and 10, the team finished the search in the northeast corner of zone D, and continued in zone C. No target of interest was identified.

The new test hub location was recorded for later search operation via hand-held GPS as: N 61.74631° W 46.83067°. It was buried under 2.7m of snow, with its concave (inner) surface facing north-west. Its location was flagged half-way between two large clusters of flags, hopefully visible from space in high-resolution imagery.

No further search was performed as the team encountered severe weather until the end of the campaign (see paragraph 3.5.3). The final radar coverage of the ground campaign is shown in Fig. 77. It represents approximately 430 km of 1 m wide radar tracks.

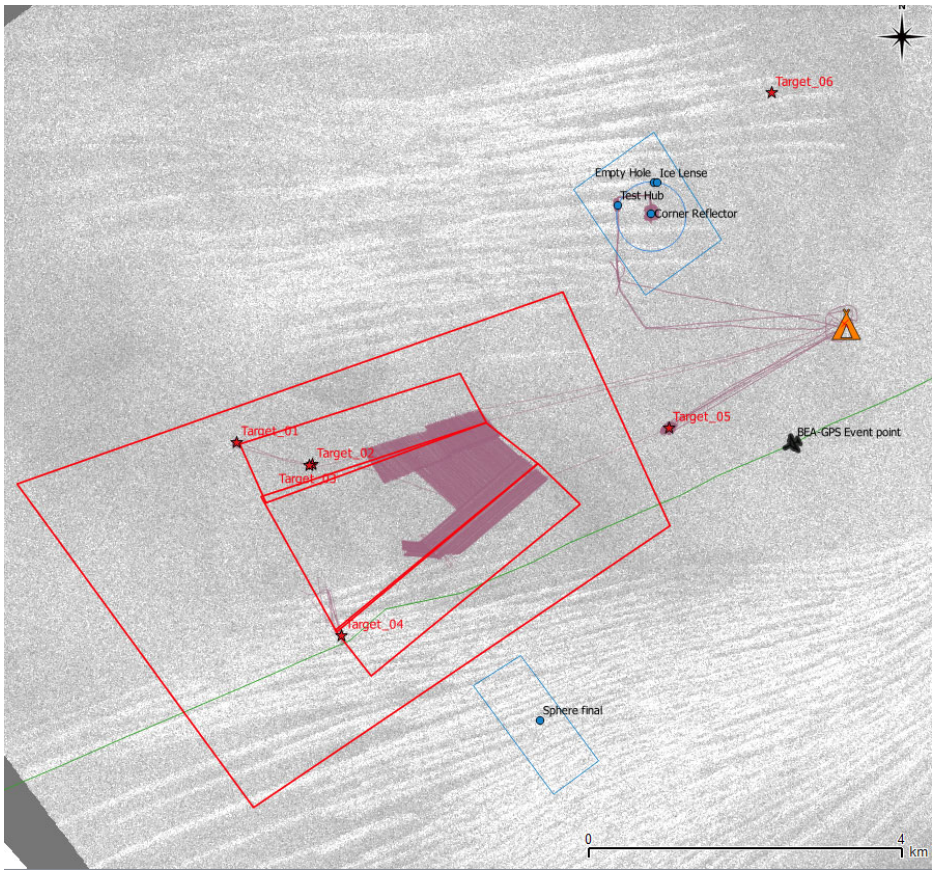

Fig. 77: ground search coverage (in purple) by GEUS team – background is a radar image in P-band

3.5.3 Weather conditions

Weather was an issue several times as the day sometimes began quite cold (-30.5°C, after sunrise). In general, the camp temperature was 5 or 10°C colder than estimated in the weather report. After a week on the camp, the team decided to shift operations to one hour later to avoid the coldest mornings and work later in the evenings. Blowing snow was also a problem as snowmobile tracks were covered too quickly so it was not possible to be sure to be on the correct line while scanning with a 1 m dense grid.

For example, May 3 began with -30 °C, 10 m/s winds, and a wind chill of -50°C. This morning was not worked due to extensive blowing snow and wind chill. When winds calmed down (by 1 pm), work commenced, on and off as weather permitted, until 10pm, with temperatures at -20°C and winds at 5 m/s. Time had also to be spent re-building snow walls for the next day's weather with winds predicted up to 17 m/s. Indeed, May 4 started with morning temperatures at -25°C and steady winds at 18 m/s, with gusts above 21 m/s. Winds held at above 15 m/s throughout the day. So no radar work was possible due to wind chill and blowing snow. Tents were even becoming buried by snow drift, and needed to be moved. During this kind of event, the team work involved reviewing images of existing radar lines and selection of dig sites.

At the end of the campaign, on May 11 and 12, the team encountered severe weather (winds up to 25 m/s and heavy snowfalls).

Some tents sustained damage (bent or broken poles, zippers opening and snow drift inside), some were abandoned in the morning. White-out conditions occurred throughout most of the day. Visibility was up to 2 to 3 m only (zero to one flag). Ropes were used to guide people from the sleeping tents to the kitchen tent. The toilet tent flipped and collapsed.

After the winds had calmed down, the team finally left the ice on May 14. Some of them went back on May 15 to finish disassembling the camp, loading the equipment into a Twin Otter and preparing the slings for the last helicopter flights.

Fig. 78: visibility in camp during snow storm with strong wind - Photo credit: GEUS

3.5.4 Ice conditions

During the field campaign, signs of large variations in snowfall were observed over relatively small spatial scales, most likely due to wind redistribution. For example, the September 2017 surface was identified at an approximate depth of 1.5m in the vicinity of the camp but this depth decreased to close to 1 m only 1.4 km away from camp. This variation in depth was also clearly visible in the radar data. GEUS identified multiple ice lenses of varying spatial extents and at different depths. The size of the ice lenses varied from a few centimeters to 60 cm vertically and often exceeded 1m horizontally. The radar data indicated that such ice lenses were common in most of the survey area and that their size and distribution varied in a seemingly random way. Finally, snow-pit studies identified clear signs of percolation with frozen ice pipes in the snowpack. The pipes are a transport mechanism for the liquid water as it percolates downwards in the snow.

4 - CONCLUSIONS

Despite the amount of work and efforts deployed for the operations described above, the fan hub fragments were not reliably detected at the end of June 2018.

The SAR operated by ONERA is an experimental technology, and its deployment over the ice sheet to detect parts buried under snow was a premiere. Despite the challenging weather conditions, no unexpected behavior or malfunctioning of the components were observed. However, due to higher background scatter noise levels and lower penetration of X band radar waves in the search zone than expected, no high confidence target was detected in the rather short time before the GEUS field campaign. ONERA finally indicated six targets to GEUS for their field campaign, with moderate confidence. More involved processing was started in order to improve the quality of the radar detections.

As the GEUS field campaign was based on target detections by the ONERA airborne campaign, once the six targets provided were looked at with no result, it had to be reconfigured into a systematic search campaign. Unfortunately, the GPR proved to be an inadequate sensor for a systematic search. Even with 430 km of search tracks analyzed, it could not be certified that if the part had laid under those tracks, it would have been detected.

These pieces of information were closely analyzed and led to additional work being considered.

5 - FURTHER WORK

ONERA continued to process the radar images acquired during the GREENSAR operation after having headed back to France. In November 2018, the process was still ongoing, as they were taking advantage of bigger computation capabilities in their facilities than the ones that they came with to Greenland. New specific algorithms made it possible to detect the test hub in the X band, which was a promising result, compared to what was deemed possible just after the field campaign.

The team considered it was necessary to test new sensors with a larger swath and a more certain response, for potential new ground searches, later on in 2019.

REFERENCES

Benson, C. S. (1962). Stratigraphic studies in the snow and firn of the Greenland.

Crider, D. (2015). Trajectory Analysis for Accident Investigation. AIAA Modeling and Simulation Technologies Conference, AIAA SciTech Forum.

DiMarzio, J. P. (2007). GLAS/ICESat 1 km Laser Altimetry Digital Elevation Model of Greenland, Version 1. . Boulder, Colorado USA - NSIDC (National Snow and Ice Data Center).

Edward Josberger, W. B. (s.d.). Fifty-Year Record of Glacier Change Reveals Shifting Climate in the Pacific Northwest and Alaska, USA. Récupéré sur USGS: http://ak.water.usgs.gov/glaciology

Joughin, I. B. (2010). Greenland Flow Variability from Ice-Sheet-Wide Velocity Mapping. Journal of Glaciology 56, 415-430.

Joughin, I. B. (2015, updated 2018). MEaSUREs Greenland Ice Sheet Velocity Map from InSAR Data, Version 2.

Paterson, W. (1994). The Physics of Glaciers (3rd ed.).

BEA

Bureau d'Enquêtes et d'Analyses
pour la sécurité de l'aviation civile

10 rue de Paris
Zone Sud - Bâtiment 153
Aéroport du Bourget
93352 Le Bourget Cedex - France
T : +33 1 49 92 72 00 - F : +33 1 49 92 72 03
www.bea.aero

www.bea.aero

Liberté • Égalité • Fraternité
RÉPUBLIQUE FRANÇAISE